Cell Biology

# PEBP1 amplifies mitochondrial dysfunction induced integrated stress response

Reviewed Preprint
v1 • December 4, 2024
Not revised

**Ling Cheng, Ian Meliala, Yidi Kong, Jingyuan Chen, Christopher G Proud, Mikael Björklund**

Centre for Cellular Biology and Signalling, Zhejiang University-University of Edinburgh (ZJU-UoE) Institute, Haining, China • Lifelong Health, South Australian Health & Medical Research Institute, Adelaide, Australia • University of Edinburgh Medical School, Biomedical Sciences, College of Medicine & Veterinary Medicine, University of Edinburgh, Edinburgh, United Kingdom



**eLife Assessment**

In this article, Cheng et al present an **important** finding that advances the understanding of mitochondrial stress response(s). The authors employed mass spectrometry-based methods in conjunction with standard molecular and cellular biology techniques to provide **compelling** evidence that phosphatidylethanolamine-binding protein 1 (PEBP1) acts as a pivotal regulator of the mitochondrial component of integrated stress response. Notwithstanding that this discovery is likely to be of significant interest to researchers across a broad spectrum of disciplines ranging from cell biology to neuroscience, it was thought that further mechanistic dissection of the role of PEBP1 in modulating integrated stress response may further strengthen this study.

https://doi.org/10.7554/eLife.102852.1.sa4

## Abstract

Mitochondrial dysfunction is involved in numerous diseases and the aging process. The integrated stress response (ISR) serves as a critical adaptation mechanism to a variety of stresses, including those originating from mitochondria. By utilizing thermal proteome profiling (TPP), we uncovered that phosphatidylethanolamine-binding protein 1 (PEBP1), also known as Raf kinase inhibitory protein (RKIP), is thermally stabilized by stresses which induce mitochondrial ISR. Depletion of PEBP1 impaired mitochondrial ISR activation by reducing eIF2α phosphorylation and subsequent ISR gene expression, which was independent of PEBP1's role in inhibiting the RAF/MEK/ERK pathway. Consistently, overexpression of PEBP1 potentiated ISR activation by heme-regulated inhibitor kinase (HRI), the principal eIF2α kinase in the mitochondrial ISR pathway. Real-time interaction analysis using luminescence complementation in live cells revealed an interaction between PEBP1 and eIF2α, which was disrupted by eIF2α S51 phosphorylation. These findings suggest a role for PEBP1 in amplifying mitochondrial stress signals, thereby facilitating an effective cellular response to mitochondrial dysfunction. Therefore, PEBP1 may be a potential therapeutic target for diseases associated with mitochondrial dysfunction.

## Introduction

Effective communication between mitochondria and the cytosol is vital for cellular and systemic homeostasis [1, 2]. A wide range of chronic diseases from neurodegeneration to type 2 diabetes [3] and even many spaceflight health risks [4] are associated with mitochondrial dysfunction. It therefore seems imperative for cells to have mechanisms to sense, integrate and respond appropriately to mitochondrial stresses. In mammalian cells, mitochondrial dysfunction elicits an integrated stress response (ISR) in the cytosol. The main function of the ISR is to manage cellular stress and to restore homeostasis, although depending on the intensity and the duration of the stress, the ISR can also induce cell death [5–11]. ISR can be triggered by various insults including deprivation of amino acids or heme, ER stress and viral infections, each of which activates one of the four eIF2α kinases, GCN2, HRI, PERK and PKR respectively, leading to the phosphorylation of eukaryotic translation initiation factor 2α (eIF2α), encoded by the *EIF2S1* gene [5]. Phosphorylation of eIF2α leads to inhibition of overall translation but promotes preferential translation of specific mRNAs, such as that encoding ATF4, a transcription factor regulating redox and amino acid metabolism [12].

While the core cytoplasmic components of ISR have been known for many years, the mechanisms relaying mitochondrial stress signals to cytoplasm to induce ISR are only beginning to be identified [6–9]. Recently, a proteolytic signaling cascade involving the mitochondrial proteins OMA1 and DELE1 and which converges on heme-regulated kinase EIF2AK1 (HRI) mediated eIF2α phosphorylation was identified [7, 8]. Additional stress relay mechanisms and regulators are thought to exist as, even in the absence of DELE1, some mitochondrial stresses can still promote eIF2α phosphorylation [8]. Further work has demonstrated than distinct mitochondrial signals activate the ISR differentially depending on the metabolic state [9] and with variable kinetics [6]. Therefore, how mitochondrial dysfunction induces ISR remains an incompletely resolved question with substantial biomedical potential [3].

Genetic screens have been instrumental in identifying genes and pathways related to mitochondrial stress signals [7, 8, 13], but they may not fully capture the dynamic and complex nature of biological regulation. Thermal proteome profiling (TPP) is a biophysical method that measures the thermal stability of proteins in cells or cell lysates [14–18]. In this assay, cells grown under different conditions are exposed to non-physiological temperatures that induce protein unfolding and precipitation. The amount of soluble protein remaining at each temperature is quantified and used an indicator of the physiological or pathological cell state. This is because thermal stability of proteins is influenced by interactions with other proteins and ligands, such nucleic acids, lipids and metabolites. Therefore, this method can provide complementary information to that from genetic screens, proteomics and metabolomics. Furthermore, thermal stability can be informative about transitions between cell states in time scales where mRNA, total protein or metabolite levels remain largely unchanged [15].

We reasoned that thermal stability of proteins might be particularly interesting in the context of mitochondrial metabolism as temperature-sensitive fluorescent probes suggest that mitochondrial temperature in metabolically active cells is close to 50°C [19]. By combining the TPP method with multiple metabolic perturbations induced by commonly used small molecule inhibitors, we systematically studied alterations in potential interaction states of proteins upon metabolic stress as indicated by differences in protein stability. We now report that phosphatidylethanolamine-binding protein 1 (PEBP1), also known as Raf kinase inhibitory protein (RKIP) [20], is thermally stabilized upon induction mitochondrial integrated stress response. Knockdown and knockout of PEBP1 attenuated mitochondrial ISR by reducing the phosphorylation of eIF2α while the response to endoplasmic reticulum stress induced by tunicamycin was not affected. PEBP1 interacted with

eIF2α while Ser51 phosphorylation of eIF2α terminated this interaction. Our results demonstrate that PEBP1 amplifies the mitochondrial ISR thereby helping the cells to respond more robustly to mitochondrial dysfunction.

# Results

## Thermal proteome profiling identifies proteins responding to metabolic stresses

To systematically identify alterations in thermal stability of proteins after metabolic perturbations, we treated 143B osteosarcoma cells, a common model system to study mitochondrial functionality, with several small molecule inhibitors (**Fig. 1A**). These treatments were selected to target oxidative phosphorylation (OxPhos complex (C)I = rotenone, CIII = antimycin A, CV = oligomycin, uncoupler CCCP), glucose uptake (2-deoxyglucose), mitochondrial division (Mdivi-1) or cholesterol synthesis (rosuvastatin). We also included the CDK4/6 inhibitor palbociclib as our positive control [21]. For proteomics, we used an experimental strategy where samples treated at different temperatures are pooled [22], thereby compressing individual thermal melting curves into an area under the curve (AUC) quantity. We reasoned that treating intact cells with the drugs for only 30 min would allow us to observe rapid and direct effects related to metabolic flux and/or signaling related to mitochondrial dysfunction in the absence of major changes in protein expression levels. We lysed the drug-treated cells and heated the lysates at 12 different temperatures below and above the median proteome melting temperature (Tm), which is ~50°C in human cells [21, 23]. We pooled the 45-50°C and 51-56°C temperature samples separately and used a non-heated lysate as a reference point for thermal stabilization (**Fig. 1A**). After removing heat-denatured proteins by centrifugation, the samples were labelled with tandem mass tags (TMT10) and analyzed by mass spectrometry.

Our positive control, CDK4, was thermally stabilized upon binding of palbociclib, as expected [21] (**Fig. 1B**). CDK4, which has a Tm of ~45°C, ranked as the fifth most stabilized protein in the 45-50°C pool when comparing palbociclib treated and control cells, while in the 51-56°C pool the stabilization was not quite as strong as expected (**Fig. 1C**). Among the ~3700 proteins detected across all treatments, many proteins were identified as being thermally stabilized by one or more drugs, indicating overlap in the cellular responses to the different metabolic perturbations (**Fig. 1D**). To focus our analysis on the most significant changes regardless of whether the Tm of each protein fell within the 45-50°C or 51-56°C temperature range, we aggregated the data from each protein into a single multivariate normal observation score using Analysis of Independent Differences (AID; see methods, Table S1). This statistical analysis ranked the proteins into the most likely thermally shifted ones using a single number. For example, CDK4 was ranked as the third most stabilized protein in palbociclib treated cells (**Fig. 1C**, Table S1).

## Mitochondrial ISR induction occurs concomitant with thermal stabilization of PEBP1

Having validated our proteomics approach, we focused our analysis on the oligomycin treatment as this drug stabilized multiple subunits of the intended target, the mitochondrial ATP synthase (e.g., ATP5PF, **Fig. S1A**). Other proteins affected by oligomycin included BANF1, which binds DNA in an ATP dependent manner [16] and mtHSP10/HSPE1, a mitochondrial heat-shock protein, suggested to be an activator of OMA1, a stress-responsive mitochondrial protease [24]. The top hit in the oligomycin stabilized proteome was phosphatidylethanolamine-binding protein 1 (PEBP1), an abundant cytoplasmic protein in most human tissues (based on the ProteinAtlas database [25]). PEBP1, ATP5PF and HSPE1were also thermally stabilized by antimycin A (**Fig. 1E**), but not by the other drugs.

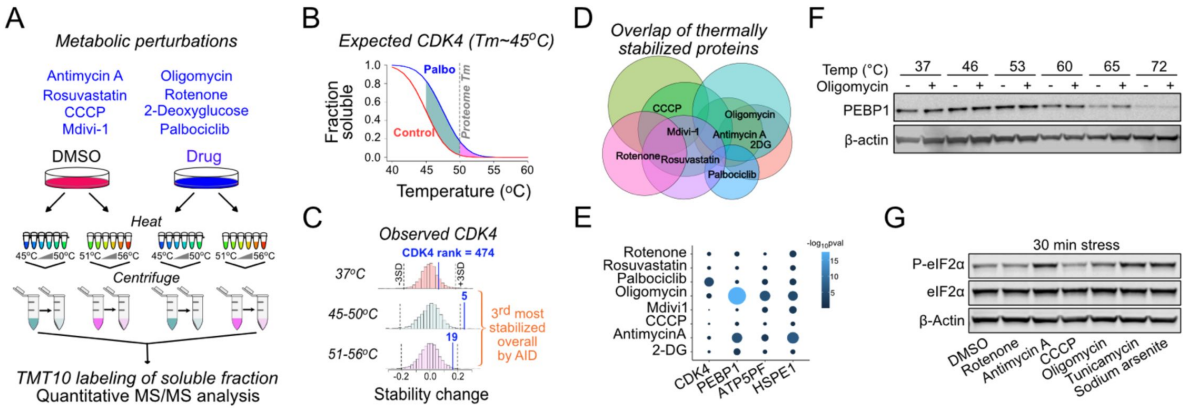


## Figure 1.

### Metabolic perturbation induced protein state changes identify PEBP1.

**(A)** Schematic of thermal proteome profiling approach. Eight different drugs, including CDK4/6 inhibitor as the positive control, were used to target metabolism in 143B cells. After heating the samples at 12 different temperatures, temperatures below and above the global proteome melting temperature (50°C) were pooled, heat-denatured proteins removed my centrifugation and analyzed by mass spectrometry. Unheated (37°C) samples and DMSO solvent control were included. **(B)** Schematic showing the expected thermal denaturation curves for control and palbociclib treated cells. The green and pink area between the curves show the integral of the thermal shift detected as difference in CDK4 protein levels in the lower and higher temperature pool. **(C)** Histograms showing the observed CDK4 ranking in palbociclib treated cells in the pools heated at different temperature ranges. The overall ranking was obtained using the Analysis of Independent Differences (AID) multivariate analysis. **(D)**Venn diagram showing the overlap between thermally stabilized proteins with different drugs. A 5% false discovery rate was used to identify the hits. **(E)** Specificity of protein state alterations illustrated as AID scores ($-\log_{10}$pval) across different drug treatments for selected hits. Note the similarity between oligomycin and antimycin A treatments. **(F)** Validation of PEBP1 thermal stabilization by oligomycin. Western blot is representative from at least 3 experiments. **(G)** Integrated Stress Response induction after a 30 min treatment with 1μM Rotenone, Antimycin A, CCCP or oligomycin as well as 5 μM tunicamycin or 25μM sodium arsenite.

Western blot based thermal shift assay validated thermal stabilization of PEBP1 (**Fig. 1F**). To exclude the possibility that oligomycin affects PEBP1 independently of the inhibition of ATP synthase, we used bedaquiline, a structurally unrelated Complex V inhibitor. Both oligomycin and bedaquiline increased mitochondrial membrane potential and this effect was inhibited by BAM15 (used as an uncoupler) indicating inhibition of ATP synthase (**Fig. S1B**). Both oligomycin and bedaquiline stabilized PEBP1 in a thermal shift assay indicating that PEBP1 is not an ATP synthase independent off-target of oligomycin (**Fig. S1C**). Furthermore, purified recombinant PEBP1 did not display thermal stabilization in an *in vitro* thermal shift assay indicating that oligomycin does not directly bind PEBP1 (**Fig. S1D**).

Previous work has reported that oligomycin and antimycin are the most efficient electron transport chain targeting compounds in activating integrated stress response target genes [26]. A 30 min treatment that stabilized PEBP1 with antimycin A or oligomycin was also sufficient to induce eIF2α phosphorylation, the core event in the integrated stress response [5] (**Fig. 1G**). Tunicamycin and sodium arsenite, used as positive controls, induced robust eIF2α phosphorylation. Rotenone increased eIF2α phosphorylation only after 4 h while CCCP at the concentration used did not do so noticeably even at that time (**Fig. S1E**) demonstrating that the mitochondrial ISR kinetics and intensity varies depending on the inducer [6, 9]. Therefore, this data suggested that stabilization of PEBP1 occurs concomitant with induction of the mitochondrial ISR.

## Loss of PEBP1 attenuates mitochondrial ISR gene expression in cultured cells and *in vivo*

PEBP1 has not been previously linked to mitochondrial dysfunction in mammalian cells. We performed RNA sequencing with non-targeting sgRNA control KO and PEBP1 sgRNA KO cells treated with and without oligomycin for 6 h. The first dimension of the principal component analysis separated the control KO and PEBP1 KO cells (**Fig. 2A**), PEBP1 being one of the top genes with negative PCA loadings (**Fig. S2A**). The transcriptional response to oligomycin observed in control KO cells was attenuated in the PEBP1 KO cells as seen collectively in the second dimension of the PCA plot (y axis) and by single genes in a heatmap and a volcano plot (**Fig. 2B, C**). Top PCA loadings (**Fig. S2A**) and the volcano plot (**Fig. 2C**) indicated that oligomycin induced the integrated stress response (ISR) in control KO cells as expected [5–11].

While known ISR induced genes including TRIB3, ASNS, ATF4, CEBPG, DDIT3/CHOP and DDIT4 were upregulated by oligomycin in control cells, PEBP1 KO cells displayed a highly attenuated ISR response at the RNA level. In control cells, gene ontology (GO) analysis indicated enrichment of groups such as “Response of EIF2AK1 (HRI) to heme deficiency” and “Eukaryotic Translation Initiation”, consistent with activation of HRI-mediated mitochondrial integrated stress response. These GO groups were not enriched in PEBP1 KO cells (**Fig. 2D**). In contrast, thioredoxin interacting protein (TXNIP) as well as genes involved in cholesterol biosynthesis (e.g., INSIG1, HMGCS1), which are unrelated to ISR and known to be repressed by oligomycin and other OxPhos inhibitors [9], remained downregulated in both control and PEBP1 KO cells (**Fig. 2C**). Therefore, the ability of PEBP1 KO to attenuate expression of ISR genes but not cholesterol biosynthesis genes suggested that PEBP1 might be specifically involved in ISR signaling.

Consistent with the possibility of PEBP1 being involved in ISR signaling, single-cell RNAseq data from ProteinAtlas database suggested that PEBP1 is expressed similarly to ATF4, HRI and DELE1 in the liver, particularly in hepatocytes, plasma cells and Kupffer cells (**Fig. 2E**). We also analyzed a publicly available RNAseq dataset (GSE264092) of bone marrow macrophages from WT and *Pebp1* KO mice. Bone marrow is a naturally occurring low-oxygen environment [27] where mitochondrial respiration may become compromised. Gene set enrichment analysis showed that there was a tendency of OxPhos genes to be downregulated in *Pebp1* KO bone marrow macrophages (**Fig. S2H**). The cells from *Pebp1* KO animals displayed reduced expression of

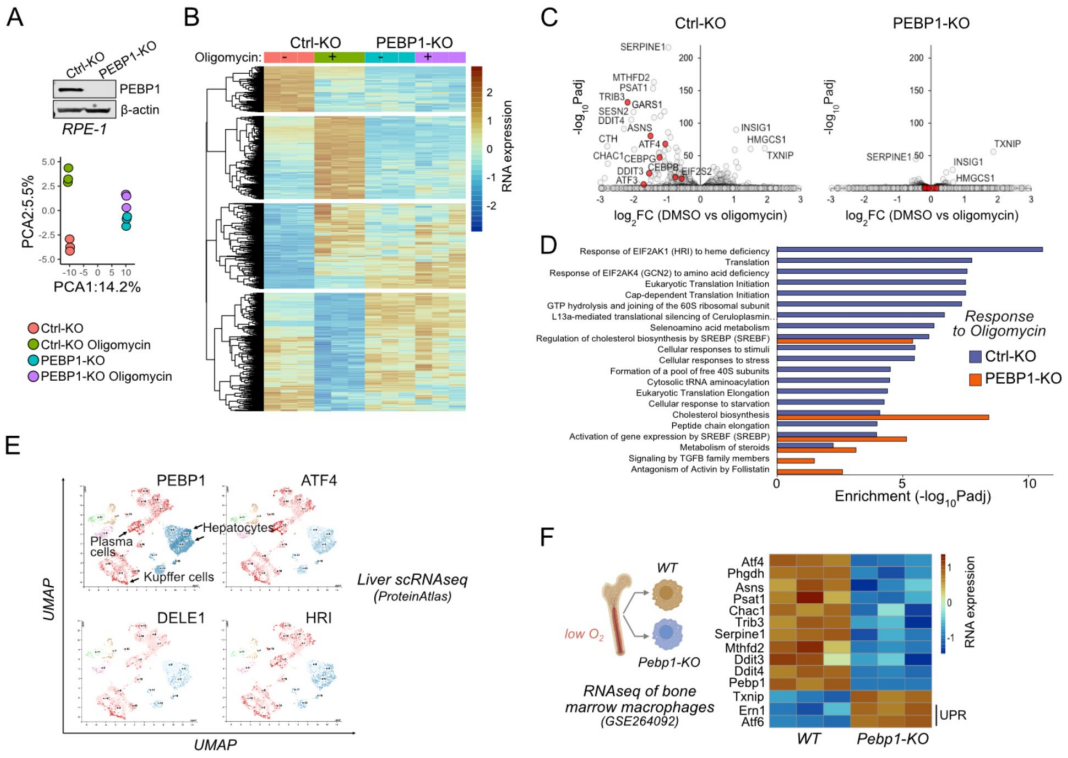


## Figure 2.

### Loss of PEBP1 attenuates ISR gene expression.

**(A)** PEBP1 expression in control and PEBP1 KO cells as well as principal component analysis of RNAseq samples treated with and without 1 μM oligomycin for 6 h. Three replicates were used for each group. **(B)** Heatmap of significantly changing genes in RNAseq. **(C)** Comparison of oligomycin induced gene expression effects using volcano plots of Ctrl and PEBP1 KO cells. Integrated stress response genes are highlighted in red. **(D)** Gene Ontology analysis of oligomycin induced responses in control KO cells (blue) and PEBP1 KO cell (red). **(E)** Comparison of PEBP1 and mitochondrial-ISR signaling component (ATF4, DELE1, HRI) expression in single-cell RNaseq from liver based on publicly available UMAP analysis from ProteinAtlas. For the names of the cell types in other clusters, see *https://www.proteinatlas.org/ENSG00000089220-PEBP1/single+cell+type/liver*. **(F)** ISR gene expression from public RNAseq data of bone marrow macrophages isolated from WT and *Pebp1* knockout mice. Unfolded protein response (UPR) genes *Ern1* and *Atf6* are also shown.

common ISR genes (**Fig. 2F**), despite upregulation of unfolded protein response genes *Ern1* (Ire1α) and *Atf6* genes. This gene expression data therefore suggest that *Pebp1* knockout *in vivo* suppresses induction of the ISR.

## PEBP1 amplifies the intensity of mitochondrial but not ER stress signaling

Western blotting indicated reduced phosphorylation of eIF2α in RPE1 cells lacking PEBP1, suggesting that PEBP1 is involved in regulating ISR signaling between mitochondria and eIF2α (**Fig. 3A**). The reduction of eIF2α phosphorylation by loss of PEBP1 was observed regardless of the approach used to activate mitochondrial ISR by targeting ATP synthase as shown by the effects of treatments with oligomycin, bedaquiline and ATP5F1A siRNA (**Fig. S2B-E**). Treatment of cells with the MEK inhibitor trametinib did not rescue eIF2α phosphorylation (**Fig. 3A**) or ISR target gene activation (**Fig. S3A,B**) although PEBP1 KO cells displayed increased ERK activation consistent with the role of PEBP1 as a RAF kinase inhibitor. Therefore, PEBP1 affects the mitochondrial ISR independently of its role in the RAF/MEK/ERK pathway [20].

We next tested if expression of PEBP1 amplifies ISR signaling by using a luciferase based ATF4 reporter assay (**Fig. 3B**). Since PEBP1 is an abundant protein, we performed these experiments in PEBP1 KO cells as its overexpression in WT cells leads to only a minor increase in total cellular PEBP1 levels. This assay demonstrated that although PEBP1 is not necessary for HRI mediated ATF4 reporter activation, it can amplify this HRI-induced signal. In addition, PEBP1 itself is not sufficient to induce reporter activity in the absence of HRI co-expression indicating that it acts as an auxiliary protein in the ISR signal transduction. PEBP1 S153D mutant, which mimics the PKC-catalyzed phosphorylation event that converts PEBP1 from a RAF inhibitor to an inhibitor of G protein coupled receptor kinase 2 (GRK2) inhibitor [28] slightly increased reporter activity, while P112E mutant which abolishes the interaction with lipooxygenases in ferroptosis [29] activated the reporter similarly to WT PEBP1. As a control, DELE1 lacking the mitochondria targeting sequence (DELE1-ι1MTS) which can directly interact with HRI in the cytoplasm to activate ISR [7] had similar effect to WT PEBP1.

Since ISR activation involves eIF2α phosphorylation and consequent downregulation of global protein synthesis, we used incorporation of the methionine analog L-homopropargylglycine (HPG) to assess the effect of PEBP1 on protein synthesis as the commonly used puromycin assay is not reliable in energy-starved cells [30]. KO of PEBP1 partially rescued the rate of protein synthesis in oligomycin treated cells but had no effect in tunicamycin treated cells (**Fig. 3C**). Taken together, the effects of PEBP1 KO on eIF2α phosphorylation, PEBP1 expression on ATF4 reporter activity and the rescue of global protein synthesis indicate that PEBP1 influences mitochondrial ISR.

The intensity and the duration of the stress determine the adaptive and cell death inducing outcomes of the ISR [31]. To test whether PEBP1 affects the amplitude or the kinetics of the stress response, we performed a time-course analysis. The phosphorylation of eIF2α induced by oligomycin was attenuated in PEBP1 KO cells at all time points (**Fig. 3D**) and concentrations (**Fig. S3C**) indicating that PEBP1 alters the amplitude; however, it did not affect the kinetics or the duration of mitochondrial stress signaling. Since the dynamic range of P-eIF2α immunoblotting is limited [32], we also checked expression of ATF4 and its transcriptional target CHOP, both of which were increased by oligomycin in control, but not in PEBP1 KO cells (**Fig. 3D**). Phosphorylation of eIF2α induced by deferoxamine mesylate (DFOM), which chelates iron and induces the ISR via the OMA1-DELE1-HRI pathway [33], was also attenuated in PEBP1 KO cells (**Fig. 3E**, S3D). Similar results were obtained by stress induced by rotenone and poly(I:C), (**Fig. S3E,F**). However, consistent with the protein synthesis assay, the phosphorylation of eIF2α induced by tunicamycin, a strong inducer of ER stress, was not prevented in PEBP1 KO cells (**Fig. 3F**, S3G). Note that in PEBP1 KO cells there was a small increase in the expression of the stress-

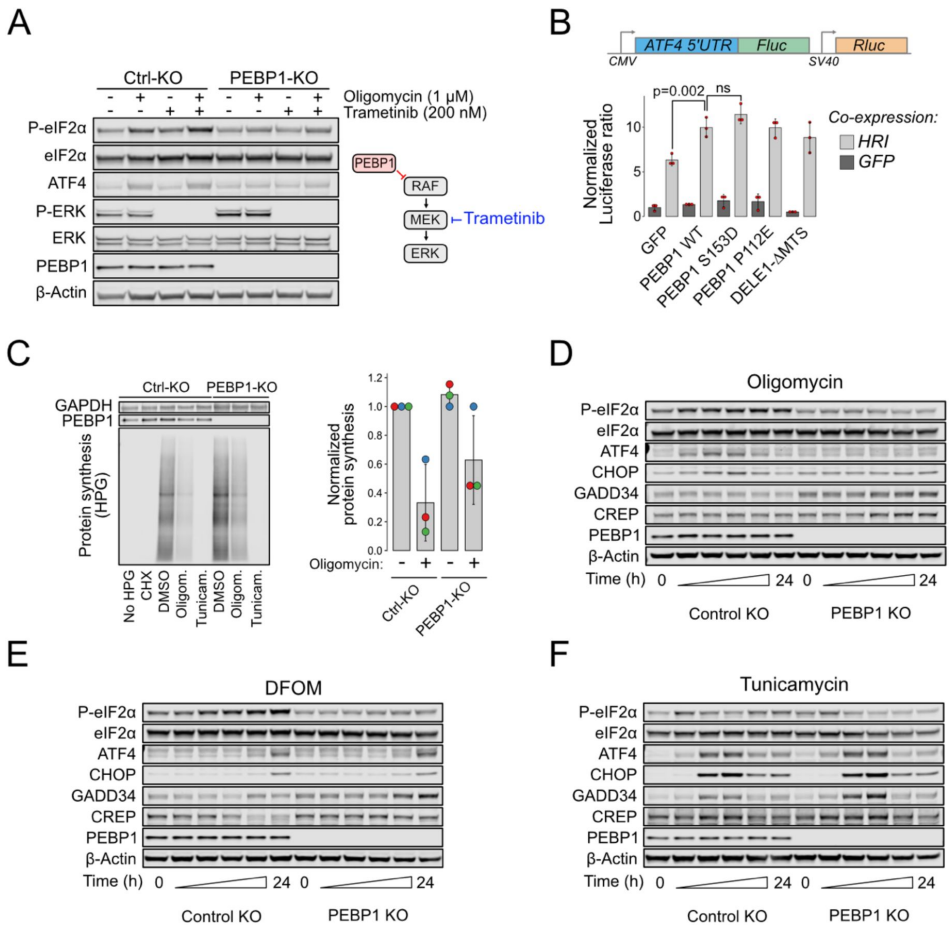


## Figure 3.

### Loss of PEBP1 attenuates HRI mediated mitochondrial signaling but not PERK mediated ER stress.

**(A)** Western blot analysis of ISR activation in RPE1 control and PEBP1 KO cells treated with and without MEK inhibitor trametinib. **(B)** ATF4 luciferase reporter assay in PEBP1 KO cells. Cells were transfected with the dual luciferase reporter (upper panel) in the presence or absence of the indicated genes (either co-expressing with GFP or HRI). Data shown in mean±SD, n=3. Statistical analysis by ANOVA followed by Tukey's post hoc test. **(C)** Effect of PEBP1on protein synthesis assayed by incorporation of a methionine analog, HPG, followed by a Click-reaction with fluorescent Azide-647. Cells were treated with 1 μM cycloheximide (CHX), 5 μM oligomycin or 5 μM tunicamycin to inhibit protein synthesis. Right panel shows quantification of oligomycin effect from three biological replicates (individual experiments highlighted with dot color). **(D)** Time-course analysis of ISR activation in RPE1 control and PEBP1 KO cells treated with 1 μM oligomycin. **(E)** Time-course of cells treated with 1 mM DFOM. **(F)** Time-course of cells treated with 1 μM tunicamycin. The specific time points in panels D-F are 0, 2, 4, 8, 16 and 24h. Western blots are representative examples from 2-3 experiments.

inducible eIF2α phosphatase subunit GADD34 (PPP1R15A) as well as the constitutively expressed PPP1R15B subunit. However, this increase in phosphatase levels could not explain the reduction of eIF2α phosphorylation in PEBP1 KO cells as Sephin-1 and Raphin-1, inhibitors of PPP1R15A and PPP1R15B, respectively, did not rescue eIF2α phosphorylation (**Fig. S3H**). Overall, these results indicate that PEBP1 is involved in amplifying the ISR to a variety of stimuli, particularly those that induce mitochondrial dysfunction.

## Loss of PEBP1 interferes with mitochondrial stress signaling without affecting OMA1 or DELE1

We next sought to understand how PEBP1 is linked to mito-ISR signaling mediated by the OMA1-DELE1-HRI pathway [7, 8]. Activation of OMA1 leads to mitochondrial fragmentation [34]. Oligomycin fragmented mitochondria in both control and PEBP1 KO cells (**Fig. 4A**). The mitochondrial oxygen consumption rate was also reduced after oligomycin addition in both control and PEBP1 KO cells. Compared to control cells, we observed only a minor reduction in basal respiration and oligomycin sensitive ATP production in PEBP1 KO cells (**Fig. 4B,C**). Mitochondrial coupling efficiency and the respiratory control ratio were also similar to control cells. There was no increase in the extracellular acidification rate (ECAR), a parameter used to measure glycolytic activity. Overall, this data indicates that PEBP1 does not have a major effect on metabolic activity in these cells.

Previous work identified that mitochondrial hyperpolarization mediates oligomycin induced ISR signaling [9]. TMRE staining confirmed that mitochondrial membrane potential was increased with oligomycin treatment, but this hyperpolarization was not reduced by PEBP1 knockdown (**Fig. 4D**), while the uncoupler BAM15 readily depolarized mitochondria. We then checked whether PEBP1 influences activation of DELE1 (**Fig. 4E**). Upon mitochondrial stress, OMA1 proteolytically cleaves and activates mitochondria-localized DELE1. DELE1-HA knock-in RPE1 cells showed the expected cleavage of DELE1 in response to oligomycin, but this cleavage was not influenced by PEBP1 knockdown (**Fig. 4F**).

## Phosphorylation modulates interaction of PEBP1 with eIF2α

PEBP1 is thought to act as a scaffold protein for regulating cellular signaling [29, 35]. Scaffolds are typically used for spatial organization of signaling components to achieve efficient and specific signal transduction [35, 36]. For example, activation of the eIF2α kinase GCN2 requires GCN1 and GCN20 as accessory proteins [12] and these proteins can be considered as scaffolds. It was also recently suggested that DELE1 oligomerization could serve as a scaffold for HRI activation [37].

Scaffold proteins typically function either stoichiometrically [38, 39] or in excess relative to the partner kinase to allow signal amplification [40]. Using data from mass-spectrometry based quantification in HeLa cells [41], roughly equimolar concentrations of PEBP1 and eIF2α were observed. Instead, PEBP1 is ~10-1000 times more abundant than any of the ISR kinases and ~6000 times more abundant than DELE1 in HeLa cells (**Fig. 5A**). Publicly available spatial transcriptomics data [42] show that PEBP1 mRNA is highly expressed in most if not all mouse tissues, particularly in the brain (**Fig. S4A**). Given the abundances of the mitochondrial ISR signaling components and the observed reduction in eIF2α phosphorylation in PEBP1 KO cells, we reasoned that among the mitochondrial-ISR signaling components, PEBP1 might most likely interact with eIF2α. However, co-immunoprecipitation assays failed to show an interaction between these proteins (data not shown). Since many protein interactions may be too weak or transient for detection by co-immunoprecipitation assay, we used NanoBiT luminescence complementation assay where a pair of interacting proteins brings the large (LgBiT) and small (SmBiT) luciferase fragments together to catalyze bioluminescence [43]. HEK293T cells expressing PEBP1-LgBiT displayed luminescence when co-transfected with eIF2α-SmBiT but not with an empty SmBiT vector (**Fig. 5B**). Phorbol ester (PMA) treatment, which leads to

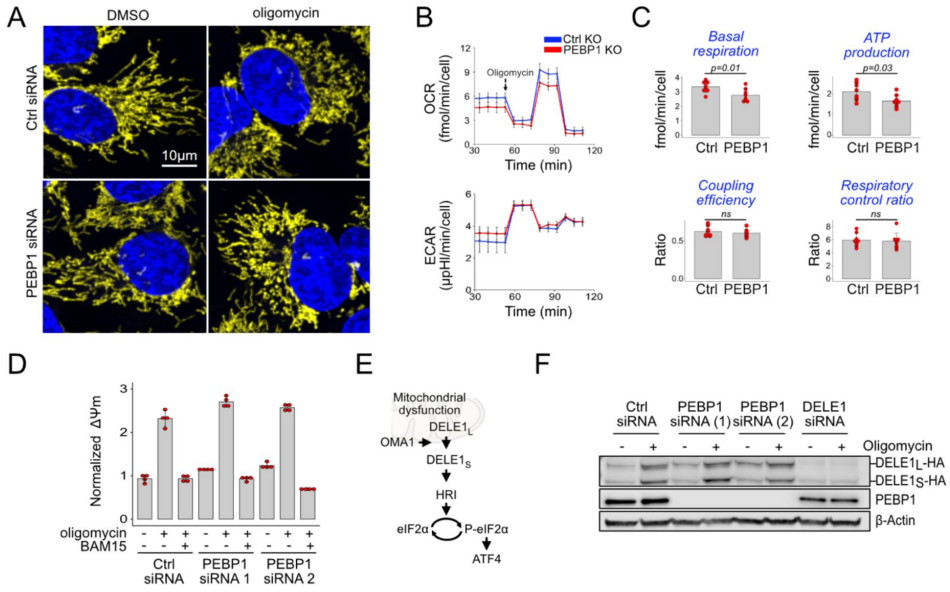


## Figure 4.

### PEPB1 does not interfere with mitochondrial OMA1-DELE1 signaling.

**(A)** A representative example of mitochondrial fragmentation in 143B cells treated with or without PEBP1 siRNA and 1 μM oligomycin. Mitochondria are shown in yellow, DNA in blue. **(B)** Seahorse oxygen consumption rate (OCR) and extracellular acidification rate (ECAR) analysis in RPE1 KO cells. **(C)** Quantification of the respiratory parameters from the Seahorse analysis. Data shown in B and C is mean±SD, n=7. The p value is from a two-sided t test. **(D)** Mitochondrial membrane potential after treating control and PEBP1 silenced 143B cells with 1 μM oligomycin or oligomycin with 0.5 μM uncoupler BAM15. **(E)** Schematic of mitochondrial stress signal transduction. **(F)** Activation of DELE1-HA in 143B endogenous knock-in cells treated with PEBP1 and DELE1 siRNAs. The long uncleaved form ($DELE1_L$-HA) and the proteolytically processed short form ($DELE1_S$-HA) are indicated.

phosphorylation of PEBP1 at Ser153, enhanced luminescence in cells transfected with WT PEBP1, but not in cells transfected with a non-phosphorylatable S153A PEBP1. This suggested a specific interaction between PEBP1-eIF2α which is enhanced by PEBP1-S153 phosphorylation. This data is consistent with the enhancement of ISR signaling by PEBP1 S153D in the ATF4 reporter assay. As a control, WB analysis demonstrated S153 phosphorylation and that expression levels of the PEBP1 and eIF2α remained unchanged by the PMA treatment (**Fig. 5B**). The phosphomimetic S153D PEBP1 mutant also displayed an increased interaction with eIF2α further supporting a specific interaction between PEBP1 and eIF2α (**Fig. S4B**). While these point mutations suggested specificity, we wanted to further demonstrate the effect of PEBP1 S153 phosphorylation on the interaction between PEBP1 and eIF2α. We therefore monitored bioluminescence changes in 5-minute intervals upon drug induced phosphorylation (**Fig. 5C**). PMA treatment of cells transfected with WT PEBP1 but not with the S153A mutant displayed increased luminescence (**Fig. 5D**).

We then tested if phosphorylation of S51 in eIF2α affects the interaction between PEBP1 and eIF2α. A phosphomimic S51D but not a S51A point mutant abolished luminescence signal suggesting that the interaction between PEBP1 and eIF2α could be terminated by S51 phosphorylation of eIF2α (**Fig. 5E**). However, this low luminescence signal was explained by loss of PEBP1-LgBiT expression as S51D eIF2α-SmBiT expression likely mimicked ISR shutting down protein synthesis. To resolve this, we performed real-time assay of PEBP1 binding to WT and S51A mutant eIF2α after inducing ISR mediated eIF2α phosphorylation with sodium arsenite. Compared to DMSO treated controls, arsenite treatment decreased the luminescence in cells expressing PEBP1 with WT eIF2α but not with the S51A mutant (**Fig. 5F**). The lack of effect in the S51A mutant suggests that lack of S51 phosphorylation of eIF2α is indeed critical for weaking the interaction between PEBP1 and eIF2alpha. The S51 phosphorylation dependent loss of protein-protein interaction is consistent with thermal stabilization of PEBP1 upon mitochondrial stress as proteins in larger complexes are generally less thermally stable. Finally, AlphaFold-Multimer analysis predicted that PEBP1 may bind eIF2α close to the S51 and the KGYID kinase recognition motif of eIF2α [44] (**Fig. 5G**), suggesting a structural basis for how PEBP1 could influence the phosphorylation of eIF2α. Taken together, these results indicate that PEBP1 acts as an amplifier of the mitochondrial integrated stress response by interacting with eIF2α (**Fig. 5H**).

## Discussion

How the intensity and duration of a stress determine the cellular stress response is complex and remains incompletely characterized. Here we have identified that Phosphatidylethanolamine-binding protein 1 (PEBP1) amplifies the integrated stress response following mitochondrial dysfunction, but not other inducers of the ISR. Loss of PEBP1 reduced the cytoplasmic integrated stress response as measured by eIF2α phosphorylation upon mitochondrial stress induced by oligomycin or iron chelation, both of which are mediated by the OMA1-DELE1-HRI pathway [33]. Importantly, PEBP1 depletion did not directly affect OMA1-DELE1-HRI pathway or repression by oligomycin of genes involved in the cholesterol synthesis pathway [9], indicating that PEBP1 is not a general mediator of the effects of OxPhos inhibition. Instead, PEBP1 dynamically interacted with eIF2α suggesting a direct and specific role in modulating ISR.

Our findings raise the question ‘why do cells utilize an additional protein, PEBP1, for mitochondrial ISR activation?’. PEBP1 did not influence tunicamycin induced stress, which is mediated by the eIF2α kinase PERK. Compared to tunicamycin, mitochondrial stress signals seem to be relatively weak activators of the ISR. For example, at least in the cell types used here, oligomycin caused a less severe inhibition of global protein synthesis and weaker ATF4 induction than tunicamycin. This may reflect differential needs for stress management, where it may be more important to handle mitochondrial stress through HRI mediated mitophagy which does not require ATF4 [45]. Therefore, we propose that PEBP1 may be required for amplifying weak

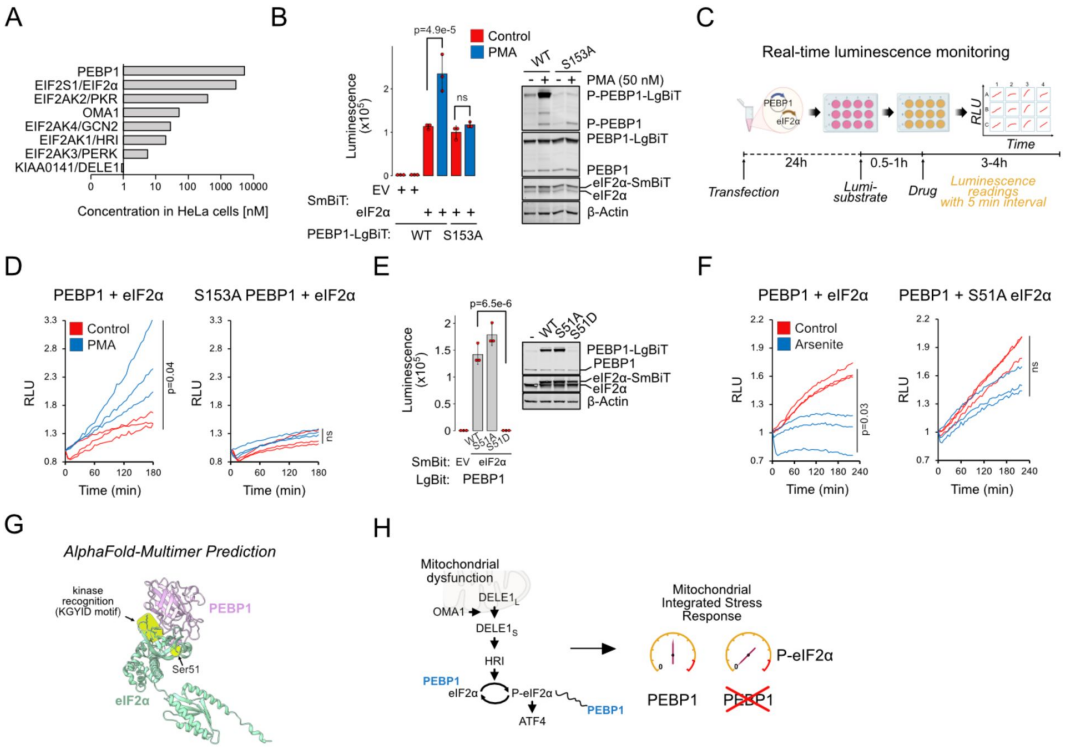


## Figure 5.

### Phosphorylation modulates interaction of PEBP1 with eIF2α.

**(A)** Protein concentrations for PEBP1 and ISR components in HeLa cells based on ref. [41]. Note the log10 scale. **(B)** Nanobit interaction assay for PEBP1 and eIF2α in 293T cells. Cells were transfected with the indicated constructs; after 24h, cells were treated with and without 50 nM PMA for 4h before adding luciferase substrate. Right panel shows the expression levels in cells transfected with WT and S153A PEBP1-LgBiT. Data is representative of three independent biological experiments. **(C)** Schematic of the real-time interaction monitoring. **(D)** Real-time analysis of PEBP1 phosphorylation dependent interaction with eIF2α using WT and S153A PEBP1. Cells were treated with 50 nM PMA. The red and blue traces show data from individual wells, n=3. **(E)** Effect of eIF2α-S51 mutations on PEBP1-eIF2α interaction. WB (right) shows expression of endogenous and exogenous eIF2α and PEBP1 levels. **(F)** Real-time analysis of PEBP1 interaction with WT and S51A eIF2α. Cells were treated with 25 μM sodium arsenite. Data is representative of three independent biological experiments with three replicate wells in each experiment. **(G)** AlphaFold prediction of the putative complex structure between PEBP1 and eIF2α. The KGYID kinase recognition motif and eIF2α-Ser51 location are indicated. **(G)** Schematic of PEBP1 in mediating mitochondrial-ISR amplification. For panels B and E, data shown is mean±SD, n=3. Statistical analysis by ANOVA, followed by Tukey's post hoc test. For panels D and F, area under curves were calculated and significance tested with two-sided t test.

stress signals, especially those that originate from mitochondria. Quantitative comparison of the signaling component amounts in HeLa cells (**Fig. 5A**) illustrates the need for substantial amplification of mitochondrial stress signals. However, efficient signal amplification should not respond to 'noise'. It was previously suggested that additional regulation of OMA1-DELE1-HRI pathway may prevent accidental stress response induction caused by proteolytically processed cytoplasmic DELE1 [8]. Signal amplification by PEBP1 may in part ensure that ISR activation results from authentic mitochondrial dysfunction. Overall, our results indicate that an efficient relay of mitochondrial stress to the cytosol via the OMA1-DELE1-HRI pathway requires PEBP1, at least in some cell types.

Mechanistically, luminescence complementation assays indicated that PEBP1 interacts with eIF2α, and that this interaction is reduced upon stress induced phosphorylation of eIF2α-S51. Although our interaction data cannot explain the increased phosphorylation of eIF2α in cells expressing PEBP1, the dynamic interaction with eIF2α and the abundance of PEBP1 relative to other components of the mitochondrial ISR pathway suggests that PEBP1 may function as a scaffold protein for efficient signal transduction and amplification (**Fig. 5H**). The current evidence, based on the observations that S153D only slightly increased ATF4 reporter activity and interaction with eIF2α in the luminescence complementation assay, suggests that S153 phosphorylation of PEBP1 is not critical for amplification of mitochondrial ISR. This effectively rules out the main previously indicated mechanism of specificity in PEBP1 signaling, where S153 phosphorylation converts PEBP1 from a RAF inhibitor to a GRK2 inhibitor [28]. Consistently, induction of ISR with oligomycin, arsenite or tunicamycin did not induce notable S153 phosphorylation based on WB analysis with the phospho-specific PEBP1 antibody (data not shown).

The identified role for PEBP1 in ISR may have broad biomedical relevance as small-molecule ISR inhibitors may potentially increase both healthspan and lifespan [46]. Enhancing or prolonging phosphorylation of eIF2α using small molecules is now being explored for disorders associated with dysregulated ISR signaling [5]. For example, ISR activation is thought to be play a causative role in a wide array of cognitive and neurodegenerative disorders [47]. Amplification of mitochondrial stress signals may be particularly important in brain and other tissues with high metabolic demands and vulnerability to mitochondrial dysfunction. PEBP1 is particularly abundant in the brain, where it is known as the precursor of hippocampal cholinergic neurostimulating peptide [48]. Given the crucial role of the ISR in the hippocampus for memory formation [47, 49], it will be important to determine whether PEBP1 plays a role in this processes and thus whether PEBP1 could be targeted therapeutically in any age-related cognitive or neurodegenerative disorders.

Our study has several limitations. The use of specific cell lines and the lack of functional data from *in vivo* experiments limit the generalizability of these findings. Apart from the detected interaction with eIF2α, our analyses are not able to pinpoint the precise mechanism by which PEBP1 enhances eIF2α phosphorylation in response to mitochondrial stresses, but not during tunicamycin induced ER stress. While the eIF2α kinases are differently located in the cell - PERK on the ER, GCN2 on ribosomes, HRI cytoplasmic, it remains possible that there are also separate pools of eIF2α such as that present on mitochondria as recently identified [50]. This remains an important point for future research.

In conclusion, by identifying PEBP1 as an amplifier of mitochondrial stress signals, our study provides new insights into cytoplasmic mechanisms which ensure appropriate responses to acute mitochondrial dysfunction. These findings may have important implications for understanding mitochondrial diseases and in developing new therapeutic strategies.

# Methods

## Cell culture

143B (CRL-8303; RRID: CVCL_2270) and hTERT RPE-1 (CRL-4000; RRID: CVCL_4388) cells were obtained from ATCC. HEK293T (RRID: CVCL_0063) cells were from GeneCopoeia, Guangzhou, China. 143B, RPE1 and HEK293T cells were cultured in 10% FBS (cat.no. VIS368948, VisTech) in DMEM containing pyruvate and L-alanyl-L-glutamine (FI101-01, Transgenbiotech, Beijing). All cell lines were cultured in the presence of penicillin and streptomycin and tested negative for mycoplasma.

## siRNA silencing

For siRNA knockdown, 143B or RPE1 cells (50,000 cells/ml) were plated in 6-well plates (2 ml/well) the day before Transfection. 25 nM SiRNA was transfected using Lipofectamine 3000 (L3000-015, ThermoFisher) prepared in OptiMEM medium (ThermoFisher). After 48 h, cells (60,000 cells/ml) were reseeded into 6-well plates (2 ml/well) for drug treatment. The following sequences were synthesized by Tsingke (Beijing) and used for the experiments. A proprietary non-targeting siRNA (Cat.No TSGXS101) from Tsingke was used as a negative control.

| | Forward Primer Sequence (5'- 3') | Reverse Primer Sequence (5' -3') |
|---|---|---|
| siDELE1-1 | CAGCGACCUGACAGUUACA(dT)(dT) | UGUAACUGUCAGGUCGCUG(dT)(dT) |
| siPEBP1-1 | GCACAGUCCUCUCCGAUUA(dT)(dT) | UAAUCGGAGAGGACUGUGC(dT)(dT) |
| siPEBP1-2 | GAUUCAGGGAAGCUCUACA(dT)(dT) | UGUAGAGCUUCCCUGAAUC(dT)(dT) |
| siATP5F1A-1 | GAUCAUCUAUGACGACUUA(dT)(dT) | UAAGUCGUCAUAGAUGAUC(dT)(dT) |

## CRISPR/Cas9

Knockout (KO) cell lines were generated by transfecting RPE1 cells with the plasmid pLentiCRISPRV2 (A gift from Feng Zhang, Addgene, #52961; RRID: Addgene_52961) containing the sgRNAs. Puromycin selection was started 24 h after transfection and continued for 7 days after which the selection medium was replaced with normal culture medium, and the cells cultured for 2-3 days before diluting ~1 cell/100 µl in a 96-well plate. Wells with single clones were expanded and sgRNA target region sequenced. Western blotting was used to confirm the knockout.

To generate DELE1 HA -knock in cells, a combination of three different plasmids were electroporated using the Neon electroporation system (ThermoFisher) as follows: 10 µg eSpCas9(1.1)_No_FLAG_ATP1A1_G3_Dual_sgRNA (A gift from Yannick Doyon, Addgene, #86613; RRID:Addgene_86613) with the guide RNA specific for the target gene and ATP1A1, 10 µg pBM16A-backbone with a glycine and serine linker and 3×HA tag, flanked on either side by the homology arms mapping to around 250 bp upstream and downstream of the stop codon of the targeted gene and 10 µg pMK-ATP1A1_Q118RN129D plasmid as the selection marker.

Electroporation was performed at a voltage of 1400 V with 1 pulse, 30 ms width on 5 million cells in resuspension buffer R for a 100 µL Neon tip. After electroporation, the cells were cultured for 3 days after which 100µM ouabain (TargetMol) was added for 5 days. Single cell clones were obtained by limiting dilution and clones analyzed by PCR and Sanger sequencing.

Sequences for generating KO cell lines:

| | |
|---|---|
| PEBP1 KO sgRNA1 | GCATGTCACCTACGCCGGGGCGG |
| PEBP1 KO sgRNA2 | CCCGGATGCTCCCAGCAGGAAGG |
| non-targeting control sgRNA | TGAGCATTCGTAGCCCAGCA |

Sequences for endogenous HA tagging of DELE1:

| | |
|---|---|
| DELE1 KI sgRNA | GAAAGGAGTGTTGTAAGACTAGG |
| ATP1A1 sgRNA | GAGTTCTGTAATTCAGCATA |

## ATF4 reporter assay

A 363-bp fragment of the ATF4 5' untranslated region (sequence TTTCTACTTTGCC…TTTGGGGGCTGA) was cloned before firefly luciferase driven by CMV promoter in pEZX-FR01 plasmid (Genecopoeia). For transfections, 50 ng ATF4 reporter + 30 ng Flag-HRI or GFP-Flag + 70 ng untagged PEBP1, GFP-Flag or DELE1-ι1MTS overexpression plasmids were mixed with 0.15 µl Plus Reagent and 0.3 µl Lipofectamine LTX (ThermoFisher) in Optimem medium and added to each well plated with 12 000 PEBP1 KO cells/well the day before. After 24h, dual luciferase assay was performed using Dual-Lumi reagents (RG088M, Beyotime, China). Luminescence values were normalized by dividing firefly luminescence values with Renilla luciferase signal and setting ATF4 reporter activity co-transfected with GFP as 1.

## NanoBiT protein interaction assay

Full length ORFs of PEBP1 and EIF2S1 (eIF2α) were amplified from RPE1 cDNA, cloned into pcDNA3.1+ vector and tagged C-terminally with SmBiT and LgBiT [43], respectively. The LgBiT was synthesized at SynbioB (Tianjin, China). Point mutations were generated by standard site-directed mutagenesis and validated by sequencing. For transfection, 293T cells (180 000 cells/ml) were plated in white 96-well tissue culture plates (Biosharp, BS-MP-96W) in a total volume of 100 µl per well. The next day, 50 ng SmBiT and 50 ng of LgBiT expression constructs were mixed with 0.4 µl of 1mg/ml Polyethylenimine (PEI, Cat.No. 408727, Sigma-Aldrich) and added to each well. After 24 hours, cells were either left untreated or treated as indicated. Finally, 0.5µl Nano-Glo Vivazine Live Cell substrate (Promega, N2581) diluted in a total volume of 10 µl DMEM was added to each well and luminescence measured with Spark Multimode Microplate Reader (Tecan).

For the real-time monitoring, Nano-Glo Vivazine Live Cell substrate was added in 1x final concentration in 90 µl complete medium supplemented with 25 mM HEPES, pH 7.3. Cells were incubated for 30-45 min at 37°C, before adding the drugs in 10 µl volume. Luminescence was monitored with 5 min interval at 37°C using SpectraMax iD5 (Molecular Devices). Data was normalized to the initial luminescence value after adding the drugs.

## Chemical compounds

The following small molecules were used. The concentrations used are indicated separately for each data figure.

| Compound | Supplier | Catalogue Number | CAS Number |
|---|---|---|---|
| Oligomycin A | SelleckChem | S1478 | 579-13-5 |
| Bedaquiline | Aladdin | B413184 | 845533-86-0 |
| Antimycin A | Abcam | AB141904 | 1397-94-0 |
| Rotenone | Solarbio | R8130 | 83-79-4 |
| 2-deoxy-D-glucose | Macklin | D807272 | 154-17-6 |
| CCCP | Solarbio | C6700 | 555-60-2 |
| FCCP | TargetMol | T6834 | 370-86-5 |
| Rosuvastatin | Solarbio | IR0150 | 147098-20-2 |
| Mdivi-1 | Beyotime | SC8028 | 338967-87-6 |
| PD 0332991 isethionate - Palbociclib | SigmaAldrich | PZ0199 | 827022-33-3 |
| Tunicamycin | Cell signaling technology | 12819s | 11089-65-9 |
| Puromycin | BBI-lifesciences | A610593-0026 | 58-58-2 |
| BAM15 | MedChemExpress | HY-110284 | 210302-17-3 |
| Deferoxamine | SigmaAldrich | D9533 | 138-14-7 |
| Poly(I:C) | MedChemExpress | HY-107202 | 24939-03-5 |
| Sodium (meta)arsenite | SigmaAldrich | S7400 | 7784-46-5 |
| Trametinib | MedChemExpress | HY-10999 | 871700-17-3 |
| Phorbol-12-myristate-13-acetate (PMA) | Rhawn | R038872 | 16561-29-8 |

## Thermal proteome profiling

Three sub-confluent 10cm dishes of 143B were treated with each of the compounds or DMSO for 30 min. Culture medium was removed and cells washed with ice cold PBS. Each plate was lysed with 1 ml 1% NP40 (IGEPAL CA-630, Cat.No. I8896, Sigma-Aldrich) in PBS containing 1x proteinase inhibitor cocktail (Cat.No. P1008, Beyotime) and the respective drugs. Lysates were transferred to 1.5 ml tubes, centrifuged at 16 000x g for 10 min at 4℃ and the lysates from the three plates were pooled. 800 µl of each lysate was snap-frozen in liquid nitrogen as total proteome to assess any protein level changes. The remaining lysate was divided into 130 µl aliquots in 12 thin-walled PCR tubes, heated in a gradient thermal cycler (Eppendorf Mastercycler X50s) for 7 min at temperatures ranging between 45-50℃ (45.0, 45.8, 46.9, 48.0, 48.9 and 50.0℃) and 51-56℃ (51.0, 51.8, 52.9, 54.0, 54.9, 56.0℃). Equal volumes from each temperature point were combined into the 45-50℃ and 51-56℃ pools and the precipitated proteins removed by centrifugation at 16 000x g for 10 min at 4℃. The soluble supernatants were frozen in liquid nitrogen and stored at -80℃ until processed for mass spectrometry. Briefly, trypsin digested peptides were desalted and lyophilized, reconstituted in 0.5 M TEAB and labelled with TMTs. Pooled samples were run using Q ExactiveTM Plus (ThermoFisher). The MS/MS data were processed using MaxQuant (v.1.5.2.8). Tandem mass spectra were searched against human Uniprot database concatenated with reverse decoy peptides. The peptide search allowed up to 4 missing trypsin cleavages with mass tolerance for precursor ions 20 ppm in the first search and 5 ppm in the main search. Mass tolerance for fragment ions was 0.02 Da. FDR was adjusted to < 1% and minimum score for modified peptides to 40. Sample preparation and proteomics was performed at PTM-biolabs (Hangzhou, China).

## *In vitro* protein thermal shift assay

100x SYPRO Orange Protein Gel Stain (SigmaAldrich, S5692) was mixed with 1 μM purified recombinant PEBP1(Cat.No. 14582-HNAE, Sino Biological), and aliquoted it into each well of the 96-well plate in 11.5 μl total volume. 1 μl of Ferrostatin-1 and Oligomycin A were added to obtain the indicated final concentrations. Thermal melt curves were obtained using CFX96 Touch Real-Time PCR System (BioRad) using manufacturer's instructions (*https://www.bio-rad.com/sites/default/files/webroot/web/pdf/lsr/literature/Bulletin_7180.pdf*).

## RNAseq

RPE1 control KO and PEBP1 KO cells were seeded at the density of $0.6\times10^5$ cells/ml in a 10 cm dish. Cells were incubated at 37°C 5% $CO_2$ for 42 h to reach ~90% confluence. Three dishes of control and PEBP1 KO cells were treated with 1 μM Oligomycin A or equal volume of DMSO as control for 6 h, washed twice with PBS and lysed in 1 ml TRIzol on ice. Lysates were frozen in liquid nitrogen and stored at -80°C. RNA library preparation and sequencing was performed at Novogene (Beijing). Briefly, sequencing libraries were generated from total RNA using NEBNext Ultra RNA Library Prep Kit for Illumina (NEB, Cat.No. E7530L) following manufacturer's recommendations. After random fragmentation, 370~420 bp cDNA fragments were selected for paired end sequencing of 150 bp. After removal of poor-quality reads, the remaining reads were mapped against human transcriptome (Ensembl v109) using Salmon (version 1.3.0) to obtain transcript abundances. Gene level summaries were generated by *tximport*. Differential gene expression analysis for RPE1 cells (accession: GSE247262)and bone marrow macrophage (accession: GSE264092) were performed using DESeq2 from variance stabilizing transformation (vst) normalized counts. Heatmap was drawn using *pheatmap* and *ggplot2* packages in R (R version 4.2.0). For functional profiling of RNAseq data, we analysed the enrichment of differentially expressed genes (using p.adj<0.001 as the cut-off).

## Western blotting

143B or RPE1 cells (60,000 cells/ml) were plated in 6-well plates (2 ml/well) a day before treatments as indicated in each figure legend. Cells were washed with PBS and lysed with 1% NP40-PBS for WB, containing protease and phosphatase inhibitors (Beyotime, Cat.No. P1051). Equal amount of total protein (typically 20 or 30 μg/sample) were separated either on 4-12% or 4-20% SurePAGE Bis-Tris gels (Genscript) and transferred on nitrocellulose membrane (Merck Millipore) using the eBlot L1 transfer system (Genscript). Membranes were blocked with QuickBlock™ Blocking Buffer (Beyotime, P0252), incubated with primary antibodies in QuickBlock™ Primary Antibody Dilution Buffer (Beyotime, P0256) or SignalUp Western Blot sensitizer (Beyotime, P0272), followed by HRP (CST, #7074) or AlexaFluor Plus 680/800 conjugated secondary antibodies (Invitrogen, A32735 and A32729). The signals were detected with LiCOR Odyssey imager and processed and using LI-COR ImageStudio software. Only blots probed with fluorescent secondary antibodies were used for quantitation.

For protein synthesis assay using L-homopropargylglycine (HPG) and click-chemistry, RPE1 cells (50 000 cells/ml) were plated in 6-well plates (2ml/well) and cultured for 48 h. Cells were treated with oligomycin or tunicamycin for 4 h, washed once with PBS, then incubated with 1 mL/well pre-warmed L-methionine-free DMEM (D0422, Sigma-Aldrich) supplemented with 200 μM L-cystine, 2 mM L-glutamine, and 10 mM HEPES for 30 min. Oligomycin or tunicamycin were maintained during this and the subsequent period. HPG (ST2057, Beyotime) was added to 50 μM final concentration and incubated for 2 hours, cells were washed twice with ice cold PBS and lysed with 50 μl 1% NP40-PBS containing protease and phosphatase inhibitors. Equal amounts of total protein in 50 μl volume were mixed with 150 μl Click-reaction cocktail containing fluorescent Azide-647 (Beyotime, C0081) and incubated for 30 minutes at room temperature. SDS-PAGE sample

buffer was added, and the samples heated and separated on a 4-20% SDS-PAGE gel and transferred on nitrocellulose membrane. Azide-647 was visualized with the 700 nm channel on the Li-COR Odyssey.

The following antibodies were used:

| Antigen | Supplier | Cat.No. | Host species | Used dilution | Lot number | RRID |
|---|---|---|---|---|---|---|
| RKIP/PEBP1 | Abcam | ab76582 | Rabbit | 1:5000 | GR3257923-2 | AB_1267285 |
| PEBP1 Phospho-Ser153 | Diagbio | db13954 | Rabbit | 1:1000 | X0630P | AB_3371705 |
| Total OXPHOS Human WB Antibody Cocktail (to detect ATP5F1A) | Abcam | ab110411 | Mouse | 1:1000 | M5406 | AB_2756818 |
| P-eIF2α | Cell Signaling Technology | #3398 | Rabbit | 1:2000 | 8 | AB_2096481 |
| eIF2α | Cell Signaling Technology | #5324 | Rabbit | 1:2000 | 8 | AB_10692650 |
| ATF-4 | Cell Signaling Technology | #11815 | Rabbit | 1:1000 | 5 | AB_2616025 |
| β-Actin | GenScript | A00702 | Mouse | 1:3000 | 19G001892 | AB_914102 |
| HA | GenScript | A01244 | Mouse | 0.5ug/ml | H2210004-A | AB_1289306 |
| CHOP | Proteintech | 15204-1-AP | Rabbit | 1:2000 | 00132291 | AB_2292610 |
| GADD34/ PPP1R15A | Proteintech | 10449-1-AP | Rabbit | 1:2000 | 00102093 | AB_2168724 |
| CREP/PPP1R 15B | Proteintech | 14634-1-AP | Rabbit | 1:5000 | 00123911 | AB_2300036 |
| HRI | Proteintech | 20499-1-AP | Rabbit | 1:1000 | 00105271 | AB_10697665 |
| ERK1/2 | Proteintech | 11257-1-AP | Rabbit | 1:5000 | 00135728 | AB_2139822 |
| P-ERK1/2 | Proteintech | 28733-1-AP | Rabbit | 1:5000 | 00124649 | AB_2881202 |

## Quantitative RT-PCR

143B or RPE1 cells (60,000 cells/ml) were plated in 6-well plates (2 ml/well) a day before treatment. Total RNA was extracted using FastPure cell/tissue total RNA isolation Kit (Vazyme). First-strand cDNA was synthesized using the HiScript Q select RT SuperMix for qPCR (Vazyme) and qPCR was performed with ChamQ Universal SYBR qPCR master Mix (Vazyme). Fold changes in expression were calculated using $2^{-\Delta\Delta Ct}$ method normalizing the Ct values to β-actin.

The qRT-PCR Primers used were the following:

| Gene | Forward Primer Sequence (5'- 3') | Reverse Primer Sequence (5' -3') |
|---|---|---|
| DDIT4 | TGAGGATGAACACTTGTGTGC | CCAACTGGCTAGGCATCAGC |
| DDIT3 | GGAAACAGAGTGGTCATTCCC | CTGCTTGAGCCGTTCATTCTC |
| β-actin | CACCATTGGCAATGAGCGGTTC | AGGTCTTTGCGGATGTCCACGT |

## Confocal microscopy

143B cells (40,000 cells/ml) were plated in 24-well plates a day before transfection. 25 nM siRNA was transfected using Lipofectamine 3000 (L3000-015, Invitrogen), After 48 h, cells were reseeded into an eight-well chambered cover glass (Cellvis, Cat. No. C8-1.5H-N) (300 ul/well). Cells were incubated with 1 μM oligomycin A for 1 h and stained with Hoechst 33342 (1:2000 dilution, Beyotime, C1022) and Mito-Tracker Red CMXRos (1:2000, Beyotime, C1049B) for 30 min. Images were captured with a spinning-disk confocal microscopy (Nikon) equipped with 60x/1.4 numerical aperture objective. Maximum Intensity Projection images were generated using Fiji (version 2.14.0/1.54f).

## Flow cytometry

143B cells were treated for 1 h with 1 μM Oligomycin A and 0.5 μM BAM15 as indicated and stained with tetramethylrhodamine ethyl ester (TMRE, 10 nM, Solarbio, T7910) for 30 min at 37°C. Cells were trypsinized, washed twice with HBSS and analyzed with Cytek Aurora flow cytometer (Cytek Biosciences, Fremont CA). Data was processed with FlowJo software (BD Biosciences).

## Oxygen consumption rate

Oxygen consumption rate (OCR) and extracellular acidification rate (ECAR) were measured using Seahorse XFe96 Analyzer (Agilent Technologies) following the manufacturer's instructions. RPE1 cells ($1\times10^4$) of the indicated genotypes were seeded in 96-well Seahorse XFe96 cell culture microplates (Agilent Technologies) for 24 h in eight replicate wells. The culture medium was changed to Seahorse XF DMEM medium (Agilent Technologies, 103575-100) supplemented with 10 mM glucose, 1 mM pyruvate, and 2 mM L-glutamine 1 h prior to the assay by washing once with this medium followed by addition of 180 μl medium per well. Mitochondrial-stress test was performed following the standard protocol with final concentrations of 1.5 μM Oligomycin A (Selleck, Cat.No. S1478), 1.5 μM FCCP (TargetMol, T6834), and 0.5 μM rotenone (Solarbio, R8130) plus antimycin A (Abcam, AB141904) (Rot/AA). To determine the cell numbers, 5 μg/ml Hoechst 33342 (Beyotime, C1022) was added into each well after the OCR measurement and fluorescence images of the wells were taken using High-Content Imaging System IXM-C (Molecular Devices). The calculated cell numbers were imported into the Seahorse Wave Controller software (version 2.6.3.8) for data normalization.

### AlphaFold-Multimer prediction

The potential complex between eIF2α and PEBP1 (UniProt IDs P05198 and P30086, respectively) was predicted by from the amino acid sequences based on AlphaFold structure prediction model v2.3.2 implemented with ColabFold 1.5.3. at *www.tamarind.bio*. The settings used were 5 models, MSA Mode: mmseqs2_uniref_env, 3 recycles without relaxations in an unpaired_paired mode without a template. The resulting 'top' model had pLDDT=85.6, pTM=0.501 and ipTM=0.155.

### Statistical analysis

The proteome data was analyzed using Analysis of Independent Differences (AID), available from *https://gygi.med.harvard.edu/software* and *https://github.com/alex-bio/TPP*, and run locally using R environment. This software ranks most likely shifted proteins by the logarithm of the Multivariate Normal p-value "log_Multiv_Norm_pval", the descending "pval_count" (i.e., in how many pools the protein shows p value <0.05), and the decreasing magnitude of "sum_of_signs" (i.e., thermal stabilization or destabilization). For comparing responses in real-time monitoring of luminescence complementation assays, *trapz* function in *pracma* package (version 2.4.4) in R was used to calculate area under curve (AUC). For statistical comparison between the AUCs in the control and drug treated groups, two-sided t test was used. For other comparisons, ANOVA followed by Tukey's post hoc test was used.

## Data availability

RNAseq data has been deposited at the NCBI GEO repository (accession GSE247262).(***Reviewer access via *https://www.ncbi.nlm.nih.gov/geo/query/acc.cgi?acc=GSE247262*, secure token: sfspgkmklduhrad). All other data can be found as supplementary material.

## Acknowledgements

We thank Drs. Thomas Tan and David Tollervey for discussion, Chan Kuan Yoow for advice with knock-ins, Zhi Hong for manuscript comments, and the Core Facilities at the Zhejiang University-University of Edinburgh Institute for providing essential instrumentation.

## Additional information

### Funding

This work was financially supported by National Science Foundation of China (grant number 31970706). IM and JC are supported by the dual award PhD degree programme in Integrative Biomedical Sciences, while LC and YK are supported by the ZJU PhD degree programme at Zhejiang University-University of Edinburgh Institute.

### Author contributions

M.B. conceived the study, designed and interpreted the experiments, and wrote the manuscript. L.C., I.M. and Y.K. designed and conducted experiments. J.C. performed thermal proteome data analysis. C.G.P. aided in interpretation of the experiments and edited the manuscript. All authors read and approved the final manuscript.

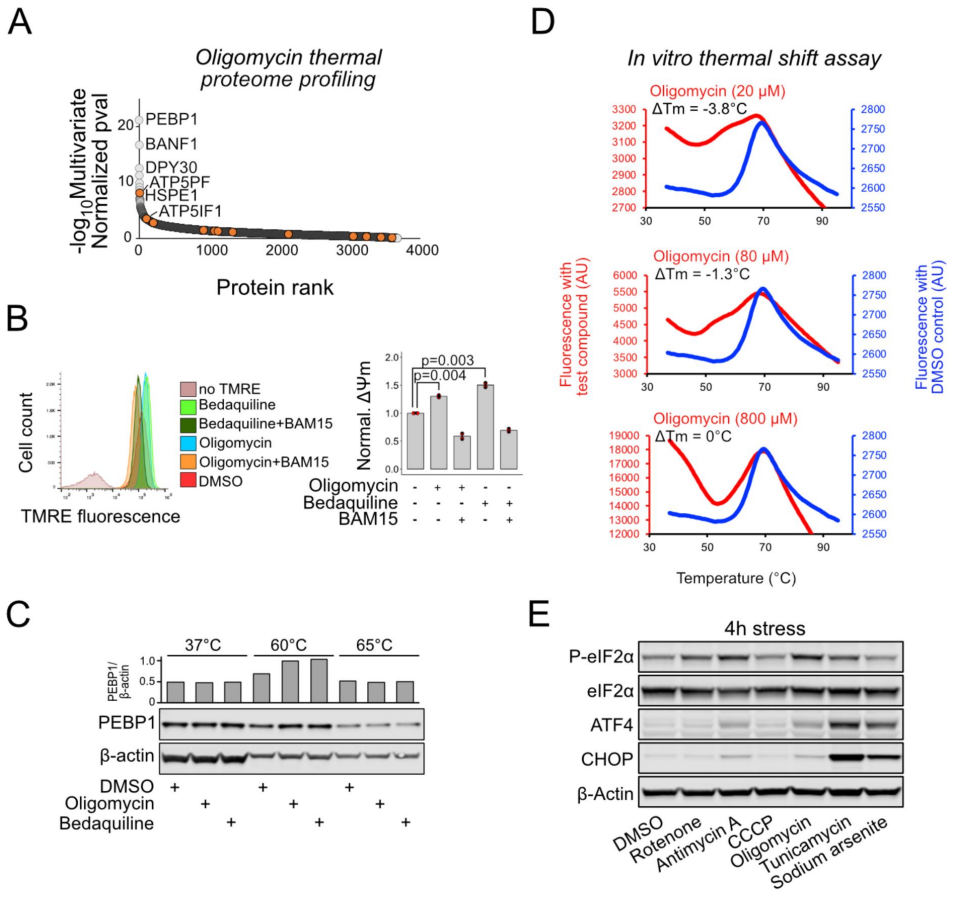


## Figure S1.

### Further characterization of PEBP1 thermal stability in cells and using purified protein.

**(A)** Ranking of oligomycin induced protein state changes based on the AID score. Mitochondrial ATP synthase subunits are indicated with orange. **(B)** Effect of ATP synthase inhibitors oligomycin and bedaquiline on mitochondrial membrane potential measured as TMRE fluorescence. 1 μM oligomycin and 5 μM bedaquiline were used. For uncoupling, 0.5 μM BAM15 was used. Right panel: Quantification of the flow cytometry data for mitochondrial membrane potential (DYm) normalized to DMSO control. Data shown in mean±SD, n=3. ANOVA, followed by Tukey's post hoc test. **(C)** Thermal shift assay using oligomycin and bedaquiline in RPE1 cells. **(D)** *In vitro* thermal shift assay with purified recombinant PEBP1. Representative melting curves for DMSO control (blue) and the indicated concentrations of oligomycin are shown together with the mean DTm between DMSO and drug treated sample from three technical replicates. **(E)** ISR induction after a 4 h treatment with the same drugs as in **Fig. 1G**.

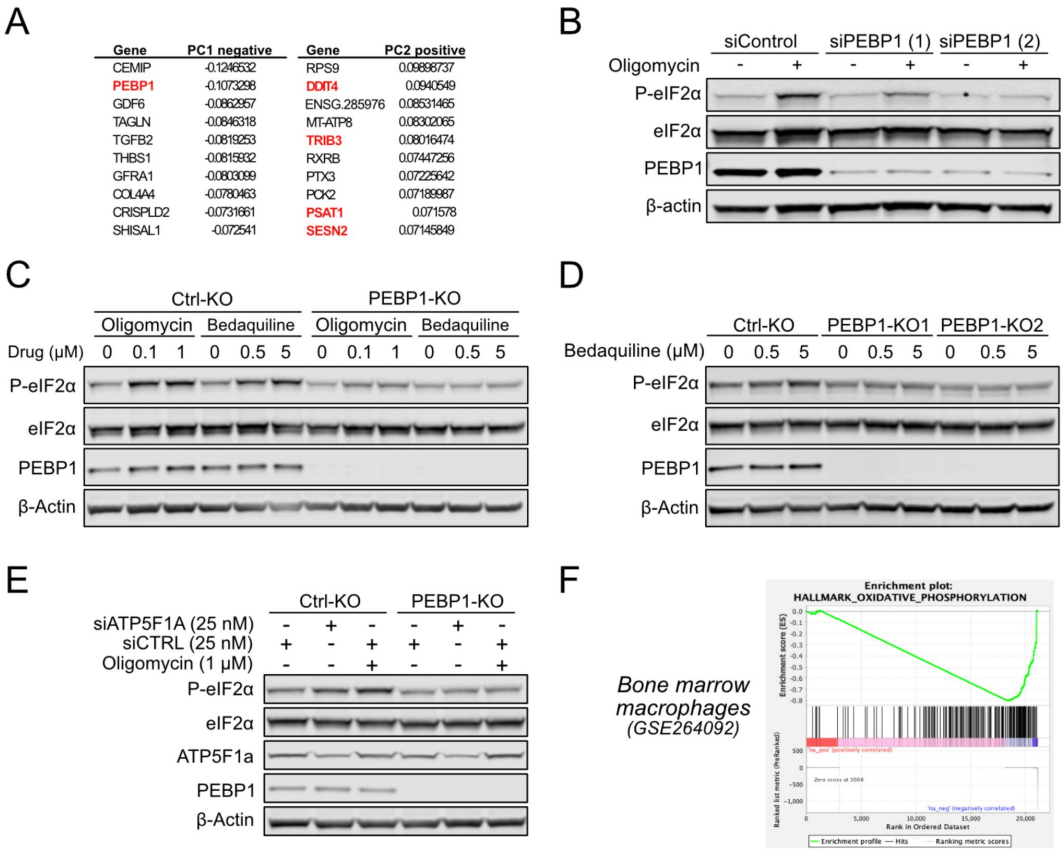


## Figure S2.

### ISR induction in control and PEBP1 KO cells is independent of the stress inducer.

**(A)** Top PCA loadings showing the individual genes with largest influence on PCA1 and PCA2 dimensions in RPE1 PEBP1 KO cell data treated with oligomycin. PEBP1 and known integrated stress response genes are highlighted in red. **(B)** WB analysis of cells treated with control and two different PEBP1 siRNA in RPE1 cells. **(C)** WB analysis of control and PEBP1 KO cells treated with oligomycin and bedaquiline at the concentrations indicated. **(D)** WB analysis of bedaquiline induced eIF2α phosphorylation using KO cell lines generated with two independent sgRNAs. **(E)** WB analysis of eIF2α phosphorylation in response to ATP synthase subunit ATP5F1A knockdown. **(F)** Enrichment of oxidative phosphorylation genes by Gene Set Enrichment Analysis (GSEA) in bone marrow macrophage RNAseq data.

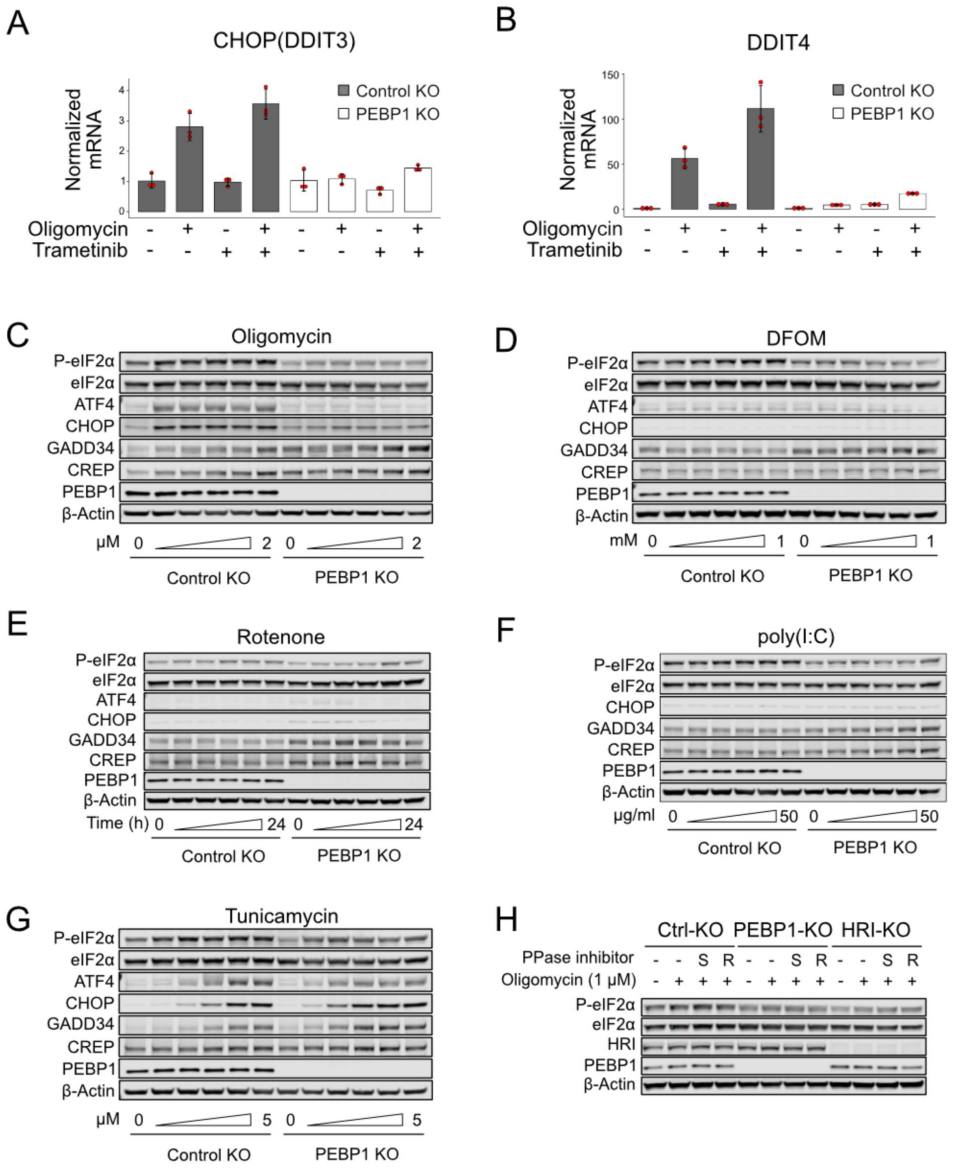


**Figure S3.**

### Characterization of PEBP1 mediated ISR.

**(A)** CHOP/DDIT3 expression by qPCR in trametinib-treated control and PEBP1 KO cells. **(B)** DDIT4 expression by qPCR in trametinib-treated control and PEBP1 KO cells. Data shown for panels C and D are mean±SD, n=3. **(C)** Dose dependent activation of ISR by oligomycin (0, 0.1, 0.25, 0.5, 1 and 2 μM final conc.) in RPE1 control and PEBP1 KO cells. **(D)** Dose-dependent activation of ISR by the iron chelator DFOM (0, 0.05, 0.1, 0.25, 0.5 and 1 mM final conc). **(E)** Time-course (0, 2, 4, 8, 16 and 24h) of cells treated with 0.5 μM rotenone. **(F)** Dose-dependent induction of ISR with poly(I:C) for 4h. The specific concentrations used were 0, 1, 5, 10, 25 and 50 μg/ml. **(G)** Dose-dependent activation of ISR with tunicamycin (0, 0.25, 0.5, 1, 2.5 and 5 μM final conc.) for 4h. **(H)** Effect of 20 μM Sephin-1 (S) and 10 μM Raphin-1 (R) phosphatase inhibitors on oligomycin induced eIF2α phosphorylation in control, PEBP1 and HRI KO cells. Phosphatase inhibitors were added 1h before adding 1 μM oligomycin, and ISR was induced for 4h before cell lysis. All experiments were repeated 2-3 times with representative data shown.

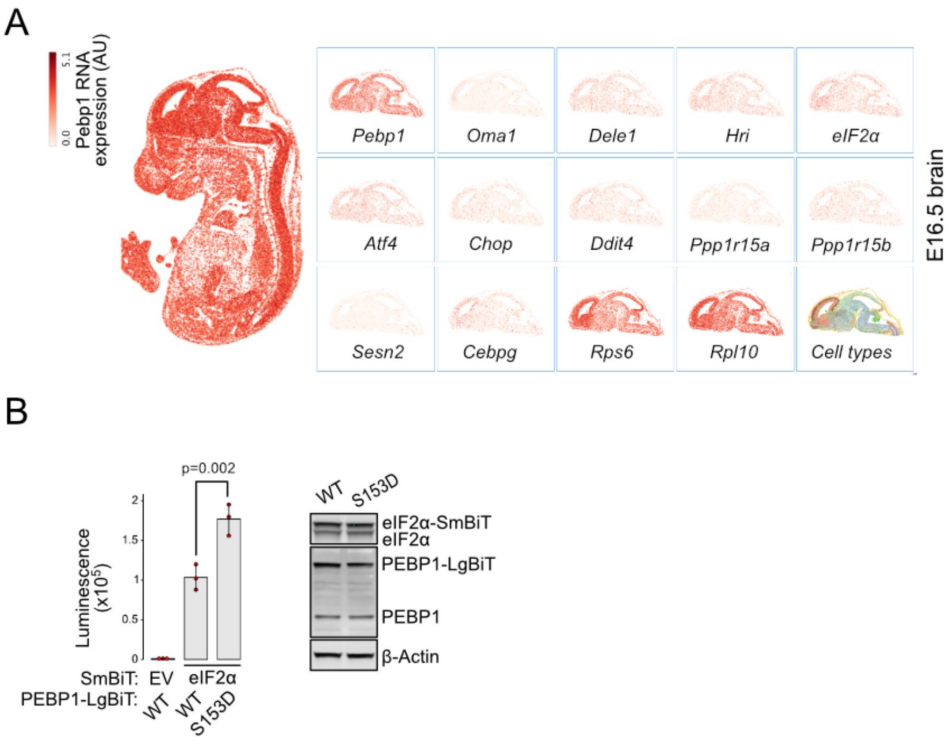


## Figure S4.

### PEBP1 and eIF2α expression and interaction.

**(A)** Expression of *Pebp1*, ISR components, and the two ribosomal subunits (*Rps6. Rpl10*) mRNAs in the mouse brain (E16.5) based on ref. [42]. **(B)** Nanobit interaction assay for PEBP1 and eIF2α in 293T cells. Cells were transfected with the indicated constructs. Luminescence was measured after 24 h. Right panel shows the expression levels in cells transfected with WT and S153D PEBP1-LgBiT. Data shown is mean±SD, n=3. Statistical analysis by ANOVA, followed by Tukey's post hoc test.

# References


1. Quiros P.M., Mottis A., Auwerx J. (2016) **Mitonuclear communication in homeostasis and stress** *Nat Rev Mol Cell Biol* **17**:213–26

2. Galluzzi L., Yamazaki T., Kroemer G. (2018) **Linking cellular stress responses to systemic homeostasis** *Nat Rev Mol Cell Biol* **19**:731–745

3. Nunnari J., Suomalainen A. (2012) **Mitochondria: in sickness and in health** *Cell* **148**:1145–59

4. da Silveira W.A., et al. (2020) **Comprehensive Multi-omics Analysis Reveals Mitochondrial Stress as a Central Biological Hub for Spaceflight Impact** *Cell* **183**:1185–1201

5. Pakos-Zebrucka K., et al. (2016) **The integrated stress response** *EMBO Rep* **17**:1374–1395

6. Condon K.J., et al. (2021) **Genome-wide CRISPR screens reveal multitiered mechanisms through which mTORC1 senses mitochondrial dysfunction** *Proc Natl Acad Sci U S A* **118**

7. Fessler E., et al. (2020) **A pathway coordinated by DELE1 relays mitochondrial stress to the cytosol** *Nature* **579**:433–437

8. Guo X., et al. (2020) **Mitochondrial stress is relayed to the cytosol by an OMA1-DELE1-HRI pathway** *Nature* **579**:427–432

9. Mick E., et al. (2020) **Distinct mitochondrial defects trigger the integrated stress response depending on the metabolic state of the cell** *Elife* **9**

10. Quiros P.M., et al. (2017) **Multi-omics analysis identifies ATF4 as a key regulator of the mitochondrial stress response in mammals** *J Cell Biol* **216**:2027–2045

11. Ryan D.G., et al. (2021) **Disruption of the TCA cycle reveals an ATF4-dependent integration of redox and amino acid metabolism** *Elife* **10**

12. Wang X., Proud C.G. (2022) **The role of eIF2 phosphorylation in cell and organismal physiology: new roles for well-known actors** *Biochem J* **479**:1059–1082

13. To T.L., et al. (2019) **A Compendium of Genetic Modifiers of Mitochondrial Dysfunction Reveals Intra-organelle Buffering** *Cell* **179**:1222–1238

14. Mateus A., et al. (2018) **Thermal proteome profiling in bacteria: probing protein state in vivo** *Mol Syst Biol* **14**

15. Dai L., et al. (2019) **Horizontal Cell Biology: Monitoring Global Changes of Protein Interaction States with the Proteome-Wide Cellular Thermal Shift Assay (CETSA)** *Annu Rev Biochem* **88**:383–408

16. Sridharan S., et al. (2019) **Proteome-wide solubility and thermal stability profiling reveals distinct regulatory roles for ATP** *Nat Commun* **10**

17. Perrin J., et al. (2020) **Identifying drug targets in tissues and whole blood with thermal-shift profiling** *Nat Biotechnol* **38**:303–308

18. Martinez Molina D., et al. (2013) **Monitoring drug target engagement in cells and tissues using the cellular thermal shift assay** *Science* **341**:. 84–7

19. Chretien D., et al. (2018) **Mitochondria are physiologically maintained at close to 50 degrees C** *PLoS Biol* **16**

20. Yeung K., et al. (1999) **Suppression of Raf-1 kinase activity and MAP kinase signalling by RKIP** *Nature* **401**:173–7

21. Miettinen T.P., et al. (2018) **Thermal proteome profiling of breast cancer cells reveals proteasomal activation by CDK4/6 inhibitor palbociclib** *EMBO J* **37**

22. Gaetani M., et al. (2019) **Proteome Integral Solubility Alteration: A High-Throughput Proteomics Assay for Target Deconvolution** *J Proteome Res* **18**:4027–4037

23. Jarzab A., et al. (2020) **Meltome atlas-thermal proteome stability across the tree of life** *Nat Methods* **17**:495–503

24. Yeung N., et al. (2023) **Role of human HSPE1 for OPA1 processing independent of HSPD1** *iScience* **26**

25. Uhlen M., et al. (2015) **Tissue-based map of the human proteome** *Science* **347**

26. Bao X.R., et al. (2016) **Mitochondrial dysfunction remodels one-carbon metabolism in human cells** *Elife* **5**

27. Spencer J.A., et al. (2014) **Direct measurement of local oxygen concentration in the bone marrow of live animals** *Nature* **508**:269–73

28. Skinner J.J., et al. (2017) **Conserved salt-bridge competition triggered by phosphorylation regulates the protein interactome** *Proc Natl Acad Sci U S A* **114**:13453–13458

29. Wenzel S.E., et al. (2017) **PEBP1 Wardens Ferroptosis by Enabling Lipoxygenase Generation of Lipid Death Signals** *Cell* **171**:628–641

30. Marciano R., Leprivier G., Rotblat B. (2018) **Puromycin labeling does not allow protein synthesis to be measured in energy-starved cells** *Cell Death Dis* **9**

31. Batjargal T., et al. (2023) **Optogenetic control of the integrated stress response reveals proportional encoding and the stress memory landscape** *Cell Syst* **14**:551–562

32. Krzyzosiak A., Pitera A.P., Bertolotti A. (2022) **An Overview of Methods for Detecting eIF2alpha Phosphorylation and the Integrated Stress Response** *Methods Mol Biol* **2428**:3–18

33. Sekine Y., et al. (2023) **A mitochondrial iron-responsive pathway regulated by DELE1** *Mol Cell* **83**:2059–2076

34. Baker M.J., et al. (2014) **Stress-induced OMA1 activation and autocatalytic turnover regulate OPA1-dependent mitochondrial dynamics** *EMBO J* **33**:578–93

35. Burack W.R., Shaw A.S. (2000) **Signal transduction: hanging on a scaffold** *Curr Opin Cell Biol* **12**:211–6

36. Good M.C., Zalatan J.G., Lim W.A. (2011) **Scaffold proteins: hubs for controlling the flow of cellular information** *Science* **332**:680–6

37. Yang J., et al. (2023) **DELE1 oligomerization promotes integrated stress response activation** *Nat Struct Mol Biol* **30**:1295–1302

38. Heinrich R., Neel B.G., Rapoport T.A. (2002) **Mathematical models of protein kinase signal transduction** *Mol Cell* **9**:957–70

39. Levchenko A., Bruck J., Sternberg P.W. (2000) **Scaffold proteins may biphasically affect the levels of mitogen-activated protein kinase signaling and reduce its threshold properties** *Proc Natl Acad Sci U S A* **97**:5818–23

40. Witzel F., Maddison L., Bluthgen N. (2012) **How scaffolds shape MAPK signaling: what we know and opportunities for systems approaches** *Front Physiol* **3**

41. Itzhak D.N., et al. (2016) **Global, quantitative and dynamic mapping of protein subcellular localization** *Elife* **5**

42. Chen A., et al. (2022) **Spatiotemporal transcriptomic atlas of mouse organogenesis using DNA nanoball-patterned arrays** *Cell* **185**:1777–1792

43. Dixon A.S., et al. (2016) **NanoLuc Complementation Reporter Optimized for Accurate Measurement of Protein Interactions in Cells** *ACS Chem Biol* **11**:400–8

44. Dey M., et al. (2005) **PKR and GCN2 kinases and guanine nucleotide exchange factor eukaryotic translation initiation factor 2B (eIF2B) recognize overlapping surfaces on eIF2alpha** *Mol Cell Biol* **25**:3063–75

45. Chakrabarty Y., et al. (2024) **The HRI branch of the integrated stress response selectively triggers mitophagy** *Mol Cell* **84**:1090–1100

46. Derisbourg M.J., Hartman M.D., Denzel M.S. (2021) **Perspective: Modulating the integrated stress response to slow aging and ameliorate age-related pathology** *Nat Aging* **1**:760–768

47. Costa-Mattioli M., Walter P. (2020) **The integrated stress response: From mechanism to disease** *Science* **368**

48. George A.J., et al. (2006) **Decreased phosphatidylethanolamine binding protein expression correlates with Abeta accumulation in the Tg2576 mouse model of Alzheimer's disease** *Neurobiol Aging* **27**:614–23

49. Sharma V., et al. (2020) **eIF2alpha controls memory consolidation via excitatory and somatostatin neurons** *Nature* **586**:412–416

50. Chakrabarty Y., et al. (2024) **The HRI branch of the integrated stress response selectively triggers mitophagy** *Mol Cell*

## Author information


**Ling Cheng**[†]
Centre for Cellular Biology and Signalling, Zhejiang University-University of Edinburgh (ZJU-UoE) Institute, Haining, China

[†]Equal contribution

**Ian Meliala**[†]
Centre for Cellular Biology and Signalling, Zhejiang University-University of Edinburgh (ZJU-UoE) Institute, Haining, China

[†]Equal contribution

**Yidi Kong**
Centre for Cellular Biology and Signalling, Zhejiang University-University of Edinburgh (ZJU-UoE) Institute, Haining, China

**Jingyuan Chen**
Centre for Cellular Biology and Signalling, Zhejiang University-University of Edinburgh (ZJU-UoE) Institute, Haining, China

**Christopher G Proud**
Lifelong Health, South Australian Health & Medical Research Institute, Adelaide, Australia

**Mikael Björklund**
Centre for Cellular Biology and Signalling, Zhejiang University-University of Edinburgh (ZJU-UoE) Institute, Haining, China, University of Edinburgh Medical School, Biomedical Sciences, College of Medicine & Veterinary Medicine, University of Edinburgh, Edinburgh, United Kingdom
ORCID iD: 0000-0002-2176-681X

**For correspondence:** mikael.bjorklund.lab@gmail.com


## Editors


Reviewing Editor
**Ivan Topisirovic**
Jewish General Hospital, Montreal, Canada

Senior Editor
**K VijayRaghavan**
National Centre for Biological Sciences, Tata Institute of Fundamental Research, Bangalore, India


**Reviewer #1 (Public review):**

Summary:

In this study, the authors use thermal proteome profiling to capture changes in protein stability following a brief (30 min) treatment of cells with various mitochondrial stressors. This approach identified PEBP1 as a potentiator of Integrated Stress Response (ISR) induction by various mitochondrial stressors, although the specific dynamics vary by stressor. PEBP1 deletion attenuates DELE1-HRI-mediated activation of the ISR, independent of its known role in the RAF/MEK/ERK pathway. These effects can be bypassed by HRI overexpression and do not affect DELE1 processing. Interestingly, in cells, PEBP1 physically interacts with eIF2alpha, but not its phosphorylated form (eIF2alpha-P), leading the authors to suggest that PEBP1 functions as a scaffold to promote eIF2alpha phosphorylation by HRI.

Strengths:

The authors present a clear and well-structured study, beginning with an original and unbiased approach that effectively addresses a novel question. The investigation of PEBP1 as a specific regulator of the DELE1-HRI signaling axis is particularly compelling, supported by extensive data from both genetic and pharmacological manipulations. Including careful titrations, time-course experiments, and orthogonal approaches strengthens the robustness of their findings and bolsters their central claims.

Moreover, the authors skillfully integrate publicly available datasets with their original experiments, reinforcing their conclusions' generality and broader relevance. This comprehensive combination of methodologies underscores the reliability and significance of the study's contributions to our understanding of stress signaling.

Weaknesses:

While the study presents exciting findings, there are a few areas that could benefit from further exploration. The HRI-DELE1 pathway was only recently discovered, leaving many unanswered questions. The observation that PEBP1 interacts with eIF2alpha, but not with its phosphorylated form, suggests a novel mechanism for regulating the Integrated Stress Response (ISR). However, as they note themselves, the authors do not delve into the biochemical or molecular mechanisms through which PEBP1 promotes HRI signaling. Given the availability of antibodies against phosphorylated HRI, it would have been interesting to explore whether PEBP1 influences HRI phosphorylation. Furthermore, since the authors already have recombinant PEBP1 protein (as shown in Figure 1D), additional in vitro experiments such as in vitro immunoprecipitation, FRET, or surface plasmon resonance (SPR) could have confirmed the interaction with eIF2alpha. Future studies might investigate whether PEBP1 directly interacts with HRI, stimulates its auto-phosphorylation or kinase activity, or serves as a template for oligomerization, potentially supported by structural characterization of the complex and mutational validation.

Another point of weakness is the unclear significance of the 1.5-2x enhanced interaction with eIF2alpha upon PEBP1 phosphorylation, as there is little evidence to show that this increase has any downstream effects. The ATF4-luciferase reporter experiments, comparing WT and S153D overexpression, may have reached saturation with WT, making it difficult to detect further stimulation by S153D. Additionally, expression levels for WT and mutant forms are not provided, making it challenging to interpret the results. It would also be interesting to explore whether combined mitochondrial stress and PMA treatment further enhance the ISR.

Lastly, while the authors claim that oligomycin does not significantly alter the melting temperature of recombinant PEBP1 in vitro, the data in Figure S1D suggest a small shift. Without variance measures across replicates or background subtraction, this claim is less convincing. The inclusion of statistical analyses would strengthen the interpretation of these results.

Impact on the field:

The study's relevance is underscored by the fact that overactive ISR is linked to a broad range of neurodegenerative diseases and cognitive disorders, a field actively being explored for therapeutic interventions, with several drugs currently in clinical trials. Similarly, mitochondrial dysfunction plays a well-established role in brain health and other diseases. Identifying new targets within these pathways, like PEBP1, could provide alternative therapeutic strategies for treating such conditions. Therefore, gaining a deeper understanding of the mechanisms through which PEBP1 influences ISR regulation is highly pertinent and could have far-reaching implications for the development of future therapies.

https://doi.org/10.7554/eLife.102852.1.sa3

**Reviewer #2 (Public review):**

Summary:

In this work, Cheng et al use the TPP/MS-CETSA strategy to discover new components for the mitochondria arm of the Integrated Stress Response. By using short exposures of several drugs that potentially induce mitochondrial stress, they find significant CETSA shifts for the scaffold protein PEBP1 both for antimycinA and oligomycin, making PEBP1 a candidate for mitochondrial-induced ISR signaling. After extensive follow-up work, they provide good support that PEBP1 is likely involved in ISR, and possibly act through an interaction with the key ISR effector node EIF2a.

Strengths:

The work adds an important understanding of ISR signaling where PEBP1 might also constitute a druggable node to attenuate cellular stress. Although CETSA has great potential for dissecting cellular pathways, there are few studies where this has been explored, particularly with such an extensive follow-up, also giving the work methodological implications. Together I therefore think this study could have a significant impact.

Weaknesses:

The TPP/MS-CETSA experiment is quite briefly described and might have a too relaxed cut-off. The assays confirming interactions between PEBP1 and EIF2a might not be fully conclusive.

https://doi.org/10.7554/eLife.102852.1.sa2

**Reviewer #3 (Public review):**

Summary:

In this paper, Chang and Meliala et al. demonstrate that PEBP1 is a modulator of the ISR, specifically through the induction of mitochondrial stress. The authors utilize thermal proteome profiling (TPP) by which they identify PEPB1 as a thermally stabilized protein upon oligomycin treatment, indicating its role in mitochondrial stress. Moreover, RNA-sequencing analysis indicated that PEBP1 may be specifically modulating the mitochondrial stress-induced ISR, as PEBP1 knock-out reduces phosphorylation of eIF2α. They also show that PEBP1 function is independent of ER stress specifically tunicamycin treatment and loss of PEBP1 does affect mitochondrial ISR but in an OMA1, DELE1 independent manner. Thus, the authors hypothesized that PEBP1 interacts directly with eIF2α, functioning as a scaffolding protein. However, direct co-immunoprecipitation failed to demonstrate PEBP1 and eIF2α

potential interaction. The authors then used a NanoBiT luminescence complementation assay to show the PEBP1-eIF2a interaction and its disruption by S51 phosphorylation.

Strengths:

Taken together, this work is novel, and the data presented suggests PEBP1 has a role as a modulator of the mitochondrial ISR, enhancing the signal to elicit the necessary response.

Weaknesses:

The one major issue of this work is the lack of a mechanism showing precisely how PEBP1 amplifies the mitochondrial integrated stress response. The work, as it is described, presents data suggesting PEBP1's role in the ISR but fails to present a more conclusive mechanism.

https://doi.org/10.7554/eLife.102852.1.sa1

**Author response:**

We thank all the reviewers for their insightful comments on this work.

**Response to Reviewer #1:**

We greatly appreciate your comments on the general reliability and significance of our work. We fully agree that it would have been ideal to have additional evidence related to the role of PEBP1 in HRI activation. Unfortunately, we have not been able to find phospho-HRI antibodies that work reliably. The literature seems to agree with this as a band shift using total-HRI antibodies is usually used to study HRI activation. However, with the cell lines showing the most robust effect with PEBP1 knockout or knockdown, we are yet to convince ourselves with the band shifts we see. This could be addressed by optimizing phos-tag gels although these gels can be a bit tricky with complex samples such as cell lysates which contain many phosphoproteins.

To address the interaction between PEBP1 and eIF2alpha more rigorously we were inspired by the insights you and reviewer #2 provided. While we are unable to do further experiments, we now think it would indeed be possible to do this with either using the purified proteins and/or CETSA WB. These experiments could also provide further evidence for the role of PEBP1 phosphorylation. Although phosphorylation of PEBP1 at S153 has been implicated as being important for other functions of PEBP1, we are not sure about its role here. It may indeed have little relevance for ISR signalling.

For the in vitro thermal shift assay, we have performed two independent experiments. While it appears that there is a slight destabilization of PEBP1 by oligomycin, the ultimate conclusion of this experiment remains incomplete as there could be alternative explanations despite the apparent simplicity of the assay due the fluorescence background by oligomycin only. We now provide a lysate based CETSA analysis which does not display the same PEBP1 stabilization as the intact cell experiment. As for the signal saturation in ATF4-luciferase reporter assay, this is a valid point.

**Response to Reviewer #2:**

We strongly agree that CETSA has a lot of potential to inform us about cellular state changes and this was indeed the starting point for this project. We apologize for being (too) brief with the explanations of the TPP/MS-CETSA approach and we have now added a bit more detail. With regard to the cut-offs used for the mass spectrometry analysis, you are absolutely right that we did not establish a stringent cut-off that would show the specificity of each drug treatment. Our take on the data was that using the p values (and ignoring the fold-changes) of individual protein changes as in Fig 1D, we can see that mitochondrial perturbations display

a coordinated response. We now realize that the downside of this representation is that it obscures the largest and specific drug effects. As mentioned in the response to Reviewer #1, we now also think that it would be possible to obtain more evidence for the potential interaction between PEBP1 and eIF2alpha using CETSA-based assays.

**Response to Reviewer #3:**

Thank you for your assessment, we agree that this manuscript would have been made much stronger by having clearer mechanistic insights. As mentioned in the responses to other reviewers above, we aim to address this limitation in part by looking at the putative interaction between PEBP1 and eIF2alpha with orthogonal approaches. However, we do realize that analysis of protein-protein interactions can be notoriously challenging due to false negative and false positive findings. As with any scientific endeavor, we will keep in mind alternative explanations to the observations, which could eventually provide that cohesive model explaining how precisely PEBP1, directly or indirectly, influences ISR signalling.

> ***Recommendations for the authors:***
>
> ***Reviewer #1 (Recommendations for the authors):***
>
> *The data overall are very solid, and I would only recommend the following minor changes:*
>
> *(1) Line 187 and line 268: there is perhaps a trend towards slightly increased ATF4-luc reporter with PEBP1-S153D, but it is not statistically significant, so I would tone down the wording here.*

We now modified this part to "This data is consistent with the modest increase..." .

> *(2) The recently discovered SIFI complex (Haakonsen 2024, https://doi.org/10.1038/s41586023-06985-7) regulates both HRI and DELE1 through bifunctional localization/degron motifs. It seems like PEBP1 also contains such a motif, which suggests a potential mechanism for enrichment near mitochondria, perhaps even in response to stress. Maybe the authors could further speculate on this in the discussion.*

While working on the manuscript, we considered the possibility that PEBP1 function could be related to SIFI complex and concluded that here is a critical difference: while SIFI specifically acts to turn off stress response signalling, loss of PEBP1 prevents eIF2alpha phosphorylation. We did not however consider that PEBP1 could have a localization/degron motif. Motif analysis by deepmito (busca.biocomp.unibo.it) and similar tools did not identify any conventional mitochondrial targeting signal although we acknowledge that PEBP1 has a terminal alpha-helix which was identified for SIFI complex recognition. We are not sure why you think PEBP1 contains such a motif and therefore are hesitant to speculate on this further in the manuscript.

> *(3) Line 358: references 50 and 45 are identical.*

Thank you for spotting this. Corrected now.

> *(4) Figure S1D: it looks like Oligomycin has a significant background fluorescence, which makes interpretation of these graphs difficult - do you have measurements of the compound alone that can be used to subtract this background from the data? Based on the Tm I would say it does stabilize recombinant PEBP1, and there is no quantification of the variance across the 3 replicates to say there is no difference.*

You are right, this assay is problematic due to the background fluorescence. The measurements with oligomycin only and subtracting this background results in slightly negative values and nonsensical thermal shift curves. We now additionally show quantification from two different experiments (unfortunately we ran out of reagents for further experiments), and this quantification shows that if anything, oligomycin causes mild destabilization of recombinant PEBP1. We also used lysate CETSA assay which does not show thermal stabilization of PEBP1 by oligomycin, ruling out a direct effect. We attempted to use ferrostatin1 as a positive control as it may bind PEBP1-ALOX protein complex, and it appeared to show marginal stabilization of PEBP1.

> ***Reviewer #2 (Recommendations for the authors):***
>
> *I have a few comments for the authors to address:*
>
> *(1) The MS-CETSA experiment is quite briefly described and this could be expanded somewhat. Not clear if multiple biological replicates are used. Is there any cutoff in data analysis based on fold change size (which correlated to the significance of cellular effects), etc? As expected from only one early timepoint (see eg PMID: 38328090), there appear to be a limited number of significant shifts over the background (as judged from Figure S1A). In the Excel result file, however (if I read it right) there are large numbers of proteins that are assigned as stabilized or destabilized. This might be to mark the direction of potential shifts, but considering that most of these are likely not hits, this labeling could give a false impression. Could be good to revisit this and have a column for what could be considered significant hits, where a fold change cutoff could help in selecting the most biologically relevant hits. This would allow Figure 1D to be made crisper when it likely dramatically overestimates the overlap between significant CETSA shifts for these drugs.*

Fair point, while we focused more on PEBP1, it is important to have sufficient description of the methods. We used duplicate samples for the MS, which is probably the most important point which was absent from the original submission as is now added to the methods. We also added slightly more description on the data analysis. While the AID method does not explicitly use log2 fold changes, it does consider the relative abundance of proteins under different temperature fractions. Since the Tm (melting temperature) for each protein can be at any temperature, we felt that if would be complicated to compare fractions where the protein stability is changed the most and even more so if we consider both significance and log2FC. Therefore, we used this multivariate approach which indicates the proteins with most likely changes across the range of temperatures. To acknowledge that most of the statistically significant changes are not the much over the background as you correctly pointed out, we now add to the main text that “However, most of these changes are relatively small. To focus our analysis on the most significant and biologically relevant changes…” We also agree that it may be confusing that the AID output reports de/stabilization direction for all proteins. In general, we are not big fans of cutoffs as these are always arbitrary, but with multivariate p value of 0.1 it becomes clear that there are only a relatively small number of hits with larger changes. We have now added to the guide in the data sheet that "Primarily, use the adjusted p value of the log10 Multivariate normal pvalue for selecting the overall statistically significant hits (p<0.05 equals -1.30 or smaller; p<0.01 equals -2 or smaller)". We have also added to the guide part of the table that “Note that this prediction does not consider whether the change is significant or not, it only shows the direction of change”

> *(2) On page 4 the authors state "We reasoned that thermal stability of proteins might be particularly interesting in the context of mitochondrial metabolism as temperature-sensitive fluorescent probes suggest that mitochondrial temperature in metabolically active cells is close to 50{degree sign}C". I don't see the relevance of this statement as an*

> *argument for using TPP/CETSA. When this is also not further addressed in the work, it could be deleted.*

Deleted. We agree, while this is an interesting point, it is not that relevant in this paper.

> *(3) To exclude direct drug binding to PEBP1, a thermofluor experiment is performed (Fig S1D). However, the experiment gives a high background at the lower temperatures and it could be argued that this is due to the flouroprobe binding to a hydrophobic pocket of the protein, and that oligomycin at higher concentrations competes with this binding, attenuating fluorescence. These are complex experiments and there could be other explanations, but the authors should address this. An alternative means to provide support for non-binding would be a lysate CETSA experiment, with very short (1-3 minutes) drug exposure before heating. This would typically give a shift when the protein is indicated to be CETSA responsive as in this case.*

Agree. However, we don't have good means to perform the thermofluor experiments to rule out alternative explanations. What we can say is (as discussed above for reviewer #1, point 4) that quantification from two different experiments shows that oligomycin is does not thermally stabilizing recombinant PEBP1. To complement this conclusion, we used lysate CETSA assay which does not show thermal stabilization of PEBP1 by oligomycin. In this assay we attempted to use ferrostatin1 as a positive control as it may bind PEBP1-ALOX protein complex, and it appeared to show marginal stabilization of PEBP1. But since we lack a robust positive control for these assays, some doubt will inevitably remain.

> *(4) The authors appear to have missed that there is already a MS-CETSA study in the literature on oligomycin, from Sun et al (PMID: 30925293). Although this data is from a different cell line and at a slightly longer drug treatment and is primarily used to access intracellular effects of decreased ATP levels induced by oligomycin, the authors should refer to this data and maybe address similarities if any.*

Apologies for the oversight, the oligomycin data from this paper eluded us at it was mainly presented in the supplementary data. We compared the two datasets and find found some overlap despite the differences in the experimental details. Both datasets share translational components (e.g. EIF6 and ribosomal proteins), but most notably our other top hit BANF1 which we mentioned in the main text was also identified by Sun et al. We have updated the manuscript text as "Other proteins affected by oligomycin included BANF1, which binds DNA in an ATP dependent manner [16], and has also identified as an oligomycin stabilized protein in a previous MS-CETA experiment [23]", citing the Sun et al paper.

> *(5) The confirmation of protein-protein interaction is notoriously prone to false positives. The authors need to use overexpression and a sensitive reporter to get positive data but collect additional data using mutants which provide further support. Typically, this would be enough to confirm an interaction in the literature, although some doubt easily lingers. When the authors already have a stringent in-cell interaction assay for PEBP1 in the CETSA thermal shift, it would be very elegant to also apply the CETSA WB assay to the overexpressed constructs and demonstrate differences in the response of oligomycin, including the mutants. I am not sure this is feasible but it should be straightforward to test.*

This is a very good suggestion. Unfortunately, due to the time constraints of the graduate students (who must write up their thesis very soon), we are not able to perform and repeat such experiments to the level of confidence that we would like.

> *(6) At places the story could be hard to follow, partly due to the frequent introduction of new compounds, with not always well-stated rationale. It could be useful to have a table also in the main manuscript with all the compounds used, with the rationale for their use stated. Although some of the cellular pathways addressed are shown in miniatures in figures, it could be useful to have an introduction figure for the known ISR pathways, at least in the supplement. There are also a number of typos to correct.*

We agree that there are many compounds used. We have attempted to clarify their use by adding this information into the table of used compounds in the methods and adding an overall schematic to Fig S1G and a note on line 132 "(see Figure 1-figure supplement 1G for summary of drugs used to target PEBP1 and ISR in this manuscript). We have also attempted to remove typos as far as possible.

> *(7) EIF2a phosphorylation in S1E does not appear to be more significant for Sodium Arsenite argued to be a positive control, than CCCP, which is argued to be negative. Maybe enough with one positive control in this figure?*

This experiment was used as a justification for our 30 min time point for the proteomics. By showing the 30 min and 4 h time points as Fig 1G and Figure 1-figure supplement 1F, our point was to demonstrate that the kinetics of phosphorylation and dephosphorylation are relevant. As you correctly pointed out, the stress response induced by sodium arsenite, but also tunicamycin is already attenuated at the 4h time point. We prefer to keep all samples to facilitate comparisons.

> *(8) Page 7 reference to Figure S2H, which doesn't exist. Should be S3H.*

Apologies for the mistake, now corrected to Figure 2-figure supplement 1B.

> *(9) Finally, although the TPP labeling of the method is used widely in the literature this is CETSA with MS detection and MS-CETSA is a better term. This is about thermal shifts of individual proteins which is a very well-established biophysical concept. In contrast, the term Thermal Proteome Profiling does not relate to any biophysical concept, or real cell biology concept, as far as I can see, and is a partly misguided term.*

We changed the term TPP into MS-CETSA, but also include the term TPP in the introduction to facilitate finding this paper by people using the TPP term.

> ***Reviewer #3 (Recommendations for the authors):***
>
> *Major Issues*
>
> *(1) The one major issue of this work is the lack of a mechanism showing precisely how PEBP1 amplifies the mitochondrial integrated stress response. The work, as it is described, presents data suggesting PEBP1's role in the ISR but fails to present a more conclusive mechanism. The idea of mitochondrial stress causing PEBP1 to bind to eIF2a, amplifying ISR is somewhat vague. Thus, the lack of a more defined model considerably weakens the argument, as the data is largely corollary, showing KO and modulation of PEBP1 definitely has a unique effect on the ISR, however, it is not conclusive proof of what the authors claim. While KO of PEBP1 diminishes the phosphorylation of eIF2a, taken together with the binding to eIF2a, different pathways could be simultaneously activated, and it seems premature to surmise that PEBP1 is specific to mitochondrial stress. Could PEBP1 be reacting to decreased ATP? Release of a protein from the mitochondria in response to stress? Is PEBP1's primary role as a modulator of the ISR, or does it have a role in non-stress-related translation? A cohesive model would tie together*

> *these separate indirect findings and constitute a considerable discovery for the ISR field, and the mitochondrial stress field.*

Thank you for your assessment, we agree that this manuscript would have been much stronger by having clearer mechanistic insights. As with any scientific endeavor, we will keep in mind alternative explanations to the observations, which could eventually provide that cohesive model explaining how precisely PEBP1, directly or indirectly, influences ISR signalling.

> *(2) The data relies on the initial identification of PEBP1 thermal stabilization concomitant with mitochondrial ISR induction post-treatment of several small molecules. However, the experiment was performed using a single timepoint of 30 minutes. There was no specific rationale for the choice of this time point for the thermal proteome profiling.*

The reasoning for this was explicitly stated: "We reasoned that treating intact cells with the drugs for only 30 min would allow us to observe rapid and direct effects related to metabolic flux and/or signaling related to mitochondrial dysfunction in the absence of major changes in protein expression levels."

> *Minor Issues*
>
> *(1) In Lines 163-166 the authors state "The cells from Pebp1 KO animals displayed reduced expression of common ISR genes (Figure 2F), despite upregulation of unfolded protein response genes Ern1 (Ire1α) and Atf6 genes. This gene expression data therefore suggests that Pebp1 knockout in vivo suppresses induction of the ISR". This statement should be reassessed. While an arm of the UPR does stimulate ISR, this arm is controlled by PERK, and canonically IRE1 and ATF6 do not typically activate the ISR, thus their upregulation is likely unrelated to ISR activation and does not contribute the evidence necessary for this statement.*

Apologies for the confusion, we aimed to highlight that as there is an increase in the two UPR arms, it is more likely that ISR instead of UPR is reduced. We have now changed the statement to the following:

"The cells from Pebp1 PEBP1 KO animals displayed reduced expression of common ISR genes (Figure 2F), while there was mild upregulation of the unfolded protein response genes Ern1 (Ire1α) and Atf6 genes. This gene expression data therefore suggests that the reduced expression of common ISR genes is less likely to be mediated by changes in PERK, the third UPR arm, and more likely due to suppression of ISR by Pebp1 knockout in vivo."

> *(2) In Lines 169 and 170 the authors state "Western blotting indicated reduced phosphorylation of eIF2α in RPE1 cells lacking PEBP1, suggesting that PEBP1 is involved in regulating ISR signaling between mitochondria and eIF2α". This conclusion is not supported by evidence. A number of pathways could be activated in these knockout cells, and simply observing an increase in p-eIF2α after knocking out PEBP1 does not constitute an interaction, as correlation doesn't mean causation. This KO could indirectly affect the ISR, with PEBP1 having no role in the ISR. While taken together there is enough circumstantial evidence in the manuscript to suggest a role for PEBP1 in the ISR, statements such as these have to be revised so as not to overreach the conclusions that can be achieved from the data, especially with no discernible mechanism.*

We have now revised this statement by removing the conclusion and stating only the observation: "Western blotting indicated reduced phosphorylation of eIF2α in RPE1 cells lacking PEBP1 (Fig. 3A)."

https://doi.org/10.7554/eLife.102852.1.sa0